AN EMBEDDING FORMALISM TO STUDY THE ELECTRONIC PROPERTIES OF DISORDERED ALLOY SYSTEMS

A Thesis Submitted
in Partial Fulfilment of the Requirements
for the Degree of

DOCTOR OF PHILOSOPHY

by

SAMITA BARDHAN

to the

DEPARTMENT OF PHYSICS

INDIAN INSTITUTE OF TECHNOLOGY KANPUR

JUNE, 1990

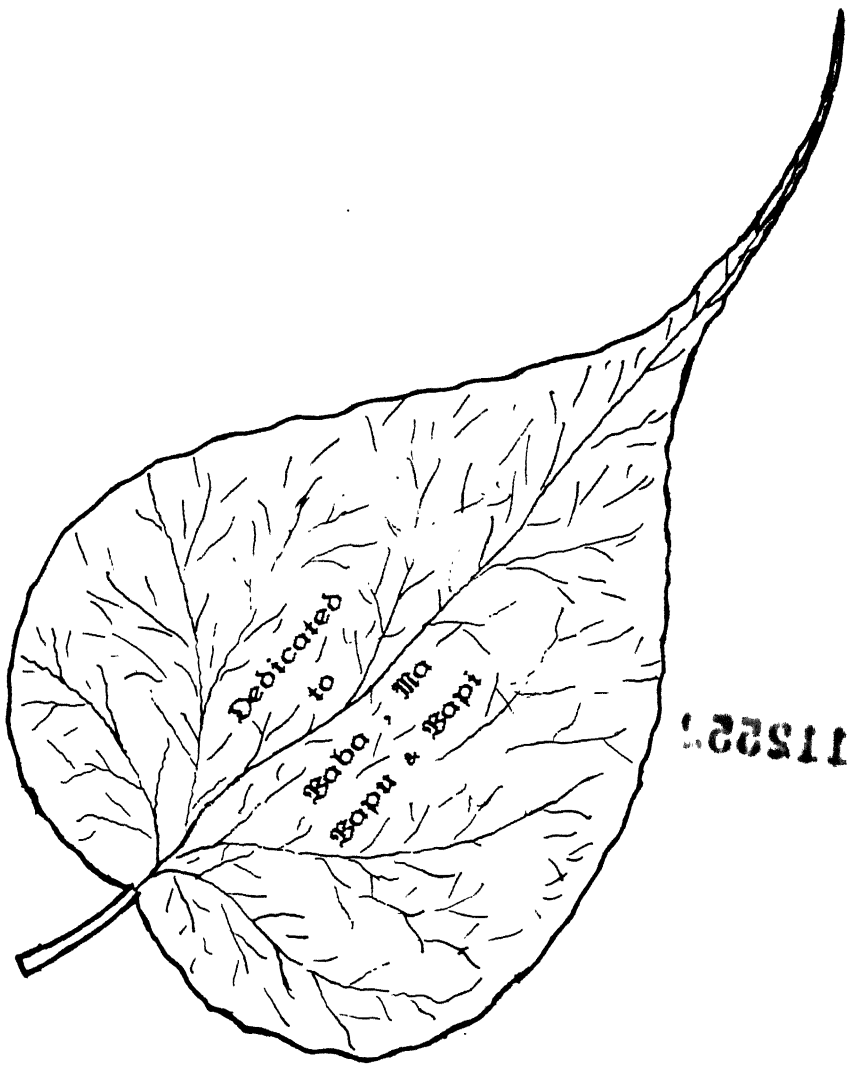
Dedicated
to
Baba, Ma
Bapu & Bapi

PHY-1990-D-BAR-EMB

CERTIFICATE

This is to certify that the work in this thesis entitled *"An embedding formalism to study the electronic properties of disordered alloy systems"* has been carried out by SAMITA BARDHAN under my supervision. No part of this work has been submitted elsewhere for a degree.

June, 1990

(ABHIJIT MOOKERJEE)
Professor,
Department of Physics,†
Indian Institute of Technology,
Kanpur 208016, India

---

† *Present address* : S.N.Bose National Centre for Basic Sciences, DB 17, Sector 1, Salt Lake City, Calcutta-700064

SYNOPSIS

Name of the Student : **Ms Samita Bardhan** Roll No. **8520965**

Degree for which submitted : **Ph.D** Department : **Physics**

Thesis Title : **An embedding formalism to study the electronic properties of disordered alloy systems**

Name of thesis supervisor : **Prof A Mookerjee**

The problem of electronic structure of random metallic alloys with its varied applications and extensions has attracted the attention of condensed matter theoreticians. The foundation of successful theory was laid by Soven (1967) and Kirkpatrick *et al* (1970) through the Coherent Potential Approximation (CPA). Soven crystallised the idea of single site CPA, with the intention of introducing complex site energies (or potentials) which characterised the effective medium in a self-consistent manner. Within multiple scattering formalism this meant that if a single exact potential is embedded in this medium, there is no extra scattering on the average.

The simplest case for which most of the CPA calculations have been done is that of binary random alloys without short-ranged order and clustering : A_cB_{1-c} where c is the concentration of A atoms in the alloy. Usually, the site energies are taken to be random (diagonal disorder) and the overlap integrals are assumed to be non-random, *i.e.*, the band widths are reasonably equal. Also it is assumed that correlated scattering from two or more sites is ignored. This is known as single site CPA or 1CPA.

This scheme has been extensively applied in both the tight-binding and the Korringa-Kohn-Rostoker (KKR) scattering approaches. It has been increasingly felt that the single site CPA appears to be inadequate in describing the effect of the clusters, extended disorder and short-ranged order.

A new formalism is proposed (in chapter II) for developing a self-consistent CPA encompassing both single potentials as well as clusters of potentials with perhaps short ranged order. This methodology is an extension to the random systems of the embedding technique introduced by Inglesfield (1977, 1978, 1981) for impurities and surfaces. This involves the partition of the Hilbert space on which the Hamiltonian is defined into two subspaces, I and II, with an interface S between them. The advantage here is that the time independent Schrödinger equation in the full Hilbert space may be solved in the smaller subspace I. The effect of the rest of the subspace, *i.e.*, (the complement of subspace I) is incorporated in the effective Hamiltonian on subspace I as a surface potential. This surface potential can be constructed from the Green function of the subspace II which satisfies the usual boundary conditions at infinity along with Neumann boundary conditions on the interface S. This Green function depends upon the potential in the subspace II. Here, subspace I is described by random binary alloy A_cB_{1-c} , whereas subspace II is described by an effective non-random potential, to be determined self-consistently applying CPA or KKR-CPA depending upon the system to be studied.

In chapter III this embedding CPA formalism is applied to the Coherent Jellium models. Here subspace II is replaced by translationally symmetric, energy dependent, site independent Coherent Jellium medium. The following problems are considered :

I. Electrons with s-symmetry, in square well potential.

II. Electrons with d-symmetry, in square well potential.

III. Electrons with s-symmetry in -V/r potential.

IV. Electrons in non-spherical potential well.

In chapter IV one dimensional Embedding-KKR formalism is developed to calculate the electron density of states of one dimensional array of flat potentials within a single well CPA and a double well CPA. Here the Green function of subspace II can be calculated from the one dimensional analog of KKR-CPA theory developed by Butler (1976) to study the electronic properties of transition metals and their alloys.

In concluding chapter further extensions and usefulness of the embedding formalism have been discussed.

ACKNOWLEDGEMENTS

Dear Prof Abhijit Mookerjee,

It is my great privilage to express my deep gratitude to you for introducing me to the physics of disordered systems. Your expert guidance and wise counsel for the past few years has been a rich experience. Apart from this academic world, working with you in 'Natayan' (The Bengali play group of the student's of IIT, Kanpur) shall always be a pleasant memory. On the personal front, I will forever recall with pleasure your gentleness and kindness towards me.

Thank you very much.

My dear Ma, Bapu and Bapi,

It would be foolish to put in words all that you have done for me. Yet, I must mention how much I appreciate your love, pride in my achievements, confidence in my abilities and constant support.

My dear Baba,

Though you are no more with me physically but you have been the driving and inspiring force behind me. Words shall never suffice to pen down coherently what you have given to me. Whatever and wherever I am to-day, it's just because of you.

Dear Prof. Tulsi Das, Prof. Batra, Prof. R. K. Thareja,

I am thankful to you for helping me at various critical points.

Dear Prof. C. K. Majumdar,

Thank you for allowing me to use the computer facility of S.N.Bose National Centre for Basic Sciences during my stay at Calcutta.

Dear Dr. R. Shankar, Dr. B. Janaki, Mr. Sanjay Deshpande,

Thank you for your cooperation in proof reading.

Dear Akhil, Debnath, Pinaki,

I can never forget your help in taking print of my thesis to give final touch to my dream.

Thank You.

Dear Mashi, Mesho, Swati, Rana,

The warm hospitality that I have received from you people during my stay at Calcutta for my thesis work shall always be memorable.

Dear Boudi, Arijit, Jayanti, Ruchira,

Thank you for treating me as one of the member of your family.

Dear friends of Natayan,

I am thankful to all of you for your sweet and sympathetic attitude.

Dear Debashish,

My warmest thank goes to you for your constant support and encouragement.

Lastly, it's my great pleasure to thank my friends Rekha, Beta, Delta, Arti, Biplab, Razee, Ranjit, Prabba Rao, Amit, Amitabha and many others for helping me at various stages of academic and non academic life during my stay at IIT Kanpur.

25th June, 1990. Samita Bardhan.

I am also thankful to Razee for giving me his path operater program which I have used after modifications to calculate the scattering path operator in one dimension.

CONTENTS

LIST OF PUBLICATIONS

I. A Self-Consistent Embedding Approach to the Electronic Structure of Random Systems,

((1989) J Phys. Condens. Matter 1, 509-518)

II. A Self-Consistent Embedding Approach to the Electronic Structures of Random Systems II: Non-Spherical Potentials,

((1990) Accepted in Int. J. Mod. Phys. B)

III. Embedding-KKR-CPA for Coherent Jellium and One Dimensional array of Flat Potentials.

(Submitted for Publication)

IV. Embedding-KKR-CPA & CCPA for One Dimensional array of flat Potentials.

(Submitted for Publication)

CHAPTER I

INTRODUCTION

Ever since the enunciation of the Bloch's theorem (1928) considerable successful effort has gone into the understanding of electronic properties of crystalline, periodic systems. Concerted and extensive effort began into the study of compositionally disordered crystalline solids, *i.e.*, random alloys, only in the late sixties. The kind of problem one encounters in random systems are also multifarious. For example

I. The understanding of various disorder linked order-disorder transitions, magnetic transitions etc.

II. The theoretical understanding of various electronic properties like density of states, optical properties, photo-emission, conductivity, dielectric response and electron related magnetic properties.

III. The understanding and description of the nature of disorder-driven localization transitions of electrons in random systems. Nature of localised states and transmission in disordered networks.

IV. The understanding of the elementary excitations in random systems such as phonons, magnons, polarons etc.

In this thesis we shall address ourselves exclusively to the understanding of the density of electronic states of random metallic alloy systems.

As we have experienced in the case of ordered systems, once the Hamiltonian model is set up, the solution of the quantum mechanics is essentially the solution of the Schrödinger equation. However, with the introduction of disorder, we face a new problem, *i.e.*, the lack of sufficient information about the sample in the Hamiltonian. The potentials which describe a disordered solid are characterised by random parameters: random in space as in quenched disordered solids or random in time as in thermally disordered systems, for example, electron in contact with phonon bath. Dirty alloys (the so called Mooij systems) at high temperature may involve both spatial and temporal disorders. A particular realisation of these parameters, either in a given sample or at an instant is what we shall call a 'configuration'of the system. Properties of a given 'configuration' may not be pertinent. We often take recourse to configuration averaging.

Before we go into the study of various methods of configuration averaging, it is important to examine why configuration average is needed and what is to be averaged.

To understand the first part, *i.e.*, why it is needed, let us consider the specific case of a crystalline substitutionally random binary alloy, in which the regular lattice sites are

randomly occupied by A or B types of atoms: random CuNi is a good example. At zero temperature the randomness is quenched and may be described by a set of random occupation variables n_i, which is determined by taking the values 0 and 1, whether a site labelled by i is occupied by an A or a B type of atom. A configuration is determined by a particular assignment of 0's and 1's to the sequence n_i. A given sample corresponds to a given configuration whereas different samples to different configurations. There are 2^N different configurations for samples containing N atoms in a binary alloy. This is a very large number for macroscopic systems. When an experimentalist talks about the characteristics of a sample he measures, he is obviously not interested in the variations between the large number of configurations. Rather he seeks average trends among his samples. If the fluctuations of a characteristic from configuration to configuration is negligible compared to the mean, then it is the configuration average which should be compared with experimentally determined characteristics.

The above discussion illustrates why configuration averaging is important. It also indicates that it is the physically measured property which should be configuration averaged: the density of states or the response functions rather than the Hamiltonian or self-energy, the diffusion probabilities rather than wave functions. Anderson (1969) gives a lucid argument on this topic to explain some of the anomalous results on the nature of the spectrum of random tight-binding Hamiltonians, which were

being proposed at that time,based on configuration averaging. Because of this, the Green function technique is far more suitable for the study of disordered systems than the Schrödinger equation approach.

The above description also clarifies that configuration averaging is a valid procedure only when the probability distribution of the property under consideration is sufficiently well behaved so that the average dominates over the higher moments, otherwise it is not profitable to talk in terms of the configuration averaging. A classic example is the intensity of star light transmitted through layered media with randomly varying refractive indices studied by Chandrasekhar (1960) and the closely related problem of the resistance of a disordered chain. Kumar and Coworker (1985,1986) have shown that the variance of the resistance of a disordered chain diverges much faster than its mean as the length of the chain increases. It is not meaningful therefore to talk about the average resistance of a very long disordered chain. There are indications that the same statement may be valid for three dimensional disordered systems, certainly on the localised regime and probably even when the Fermi energy lies just above the mobility edge.

Now it's worth-while to say something about spatial ergodicity. For a large enough system, in the limit of infinite size, all possible environments are achieved even in a single sample, as shown in figure (1.1).

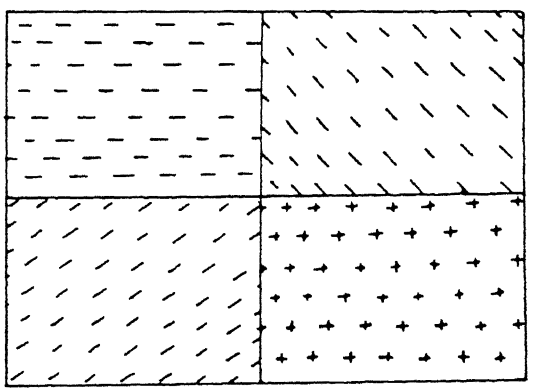

Figure 1.1 : Representation of different environment within a sample. For n $\longrightarrow \infty$,all environments are realised.

In a global-probe sample all possible environments in the sample are weighted with appropriate possibilities. A global property is thus automatically configuration averaged, even if it refers to a single sample. This sampling of the entire configuration by a spatially global probe is analogous to the sampling in statistical mechanics of all configuration space by a dynamically evolving system. Hence the name spatial ergodicity. Such global properties need not be configuration averaged all over again. This idea is implicitly behind a large body of the "large cluster" calculations involving either isolated or immersed clusters. One example is the application of the Recursion method to large disordered clusters (Haydock, 1987).

There are various mean field approaches to study the configuration averaged one and two particle Green functions for disordered systems, which are directly related to the averaged density of states and response functions. But during past two decades Coherent Potential Approximation (CPA) has been one of the main theoretical development in the area of study of electronic structure of random alloys. The simplest case for which most of the CPA calculations have been done is, that of a random binary alloy. Here the site energies are taken to be random (diagonal disorder) and the overlap integrals are assumed to be non-random, *i.e.*, there is no off-diagonal disorder. Also, it is further assumed that the correlated scattering from two or more sites is ignored. This is known as single site CPA.

The validity of the single site CPA theory has been recognised through application to various model systems as well as to realistic model Hamiltonians suitable for disordered metallic alloys. The need to go beyond 1CPA has been felt because of the following drawbacks of single site CPA :

I. It takes exactly into account only single-site scattering and correlated scattering from clusters is not accounted for,

II. The effect of potential fluctuation is automatically suppressed while doing such an average,

III. It cannot properly take into account the off-diagonal disorder in the Hamiltonian, and

IV. The vertex correction (*i.e.*, back-scattering effects) vanishes in the single band case as an artifact of short-ranged potentials in single site CPA.

The most obvious extension of the theory to overcome these limitations is to go beyond the single-site approximation by doing a general formalism so that the effects of scattering from statistically coupled clusters of various sites and that of the off-diagonal disorder could be included. Nickel and Krumhansl (1971) tried to make such generalisation using a method based on the correlated cumultant expansion to find an electronic density

of states of a one dimensional model of an alloy. Butler(1972,1973) also tried to calculate both the real and imaginary parts of the Green function using a self-consistent cluster method and both of these methods are intended to improve the CPA by going beyond the single-site approximation through making application to one-dimensional tight binding models. Such a generalisation not only posed severe analytic problems such as having discontinuities at various energies but also led to multi-valued density of states.

It was pointed out by Haydock *etal* (1972), Mookerjee (1973), Muller-Hartman (1973), Mills & Ratanavaraksa (1978) that for any real potential function, the Green function must have certain mathematical properties, called Herglotz properties. A complex function f(z) is defined as Herglotz if

i) Im f(z) < 0 for Im z < 0

ii) Singularities of f(z) lie on the real axis,

iii) $f(z) \rightarrow 1/E$ as $E \longrightarrow \infty$ (where $z = E + i0^{+}$)

In order to get physical results, Herglotzicity should be related in any approximation to the Green function. The fundamental difficulties with most theories that were proposed during the late 1960's and early 1970's as extensions of the CPA, are that they lead to approximate Green functions which are not Herglotz. It is now realised that the preservation of the Herglotz property must be one of the central considerations in

the development of a theory which includes scattering from clusters, short-ranged order, off-diagonal disorder, or the effects of positional disorder.

There have been attempts to include some of the effects of scattering from clusters of atoms, at least conceptually by using a technique called the Molecular Coherent Potential Approximation (MCPA) as discussed by Tsukada (1969) and Butler (1973). This method is a straight-forward generalisation of the CPA approach in which the lattice sites of an alloy are partitioned into cells that contain more than one lattice sites. Though in this method the Herglotz analytic property is preserved, the main objection for MCPA not being a satisfactory theory is the imposition of fictitious unit cell boundaries, and consequently, translational invariance is lost.

All the above techniques described do not prove a reliable solution to the theoretical problem of developing a self-consistent theory of the electronic states of an alloy that goes beyond the single-site approximation. The problem of going beyond the single site CPA theory has been proposed by Mills (1978) in his original studies (known as Travelling Cluster Approximation) on the problem of a Herglotz average Green function within the frame work of diagrammatic perturbation theory. But it's very cumbersome to evaluate the contribution of the higher order terms for a real three dimensional lattice by

Mookerjee (1973 a,b; 1975 a,b,c) introduced a general formalism known as Augmented Space Formalism (ASF) to calculate configuration averaging of a general function of random variables by using abstract operator formalism of quantum mechanics. He was able to establish the idea of incorporating scattering effects from statistically coupled sites in a finite size cluster, as well as the importance of off-diagonal disorder in a self-consistent manner. This formalism came out with success in producing Herglotz analytic Green function through applications to various model systems.

On the basis of the Partition theorem and the Embedding ideas of Inglesfield we develop a methodology to study the electronic structure of random systems. The equations for the Green function are confined to a finite cluster region and the influence of the rest of the region appears as a surface potential. The Herglotz analytic properties are satisfied in this case. We illustrate the methodology by applying it to a binary distribution of different single wells in a Coherent Jellium. This is the alloy generalisation of the impurity work of Inglesfield referred to in the text. This formalism is developed in most general form to take into account cluster effects as well. Extended defects and impurity clustering in a random alloy can also be taken care of with ease. This methodology is a very good technique to deal with liquid alloys with short-ranged ordering.

Here we also develop a one dimensional analog of this Embedding formalism for single as well as pair potential binary alloy impurities in a one dimensional array of flat potential wells.

CHAPTER II

AN EMBEDDING FORMALISM TO THE COHERENT POTENTIAL APPROXIMATION

One of the most powerful techniques available during the last two decades for the study of random metallic alloys is Coherent Potential Approximation (CPA). This scheme has been extensively applied both in the tight-binding and Korringa-Kohn-Rostoker (KKR) scattering approaches. But it has been extensively felt that the single site (or single potential) CPA appears to be inadequate in describing the effects of clusters, extended disorder and short-ranged order which may dominate situations like order-disorder transitions, for instance. In this chapter we wish to propose a new formalism for developing a self-consistent CPA encompassing single potential wells as well as clusters of wells and short-ranged order. This methodology is an extension to random systems of the Embedding technique introduced by Inglesfield (1971,1972, 1981) for impurities and surfaces. Before going to develop this formalism let us very briefly review Coherent Potential Approximation.

2.1 : THE COHERENT POTENTIAL APPROXIMATION

The electronic density of states per atom per spin for any system is directly related to the single particle Green function

$$n(E) = -\frac{1}{\pi N} \text{Im Tr } G(E+i0^+) \tag{2.1.1}$$

where N is the total number of atoms in the system. The Green operator (or resolvant operator) G is given by the Hamiltonian H

$$G(Z) = (ZI-H)^{-1} \tag{2.1.2}$$

where Z is a complex variable and I is the identity matrix.

For any disordered system the electronic density of states will be given by trace of the configuration averaged single particle Green operator $\langle G \rangle$. If the random variation of the potential is similar throughout the system, *i.e.*, randomness is homogeneous, then the configuration averaged electronic density of states will be

$$n(E) = -\frac{1}{\pi N} \text{Im Tr}\langle G(r,E+i0^+)\rangle \tag{2.1.3}$$

where r is any site vector in the system and the averaged Green function will be

$$\langle G \rangle = \langle (ZI-H)^{-1} \rangle. \tag{2.1.4}$$

The CPA is an attempt at an approximate evaluation of this configuration averaged Green function. It maintains the analytic features of the exact Green function and interpolates correctly between several individual limiting cases, *e.g*, the Virtual Crystal Approximation, atomic and dilute limits, weak and strong disorder limits.

There are four different approaches to the CPA as described in the extensive literature on the approximation .

I. Diagrammatic approaches using propagator and locator formalisms introduced by Yonezawa and Matsubara (1966), Yonezawa (1968), and Leath (1968,1970).

II. The effective medium approach introduced by Soven (1967).

III. Multiple scattering ideas, first introduced by Anderson and M^{c}Millan (1973), Mookerjee (1975) and Kaplan *et al* (1980).

IV. The Augmented space approach by Mookerjee (1973) and Kaplan *et al* (1980).

All different approaches yield the same final result within the single site approximation. This indicates that the single site CPA is unique. In this thesis only the effective medium approximation will be described.

2.1.1 : THE EFFECTIVE MEDIUM APPROXIMATION

The idea of the effective medium approximation (Soven 1967) gives a simple physical insight into the CPA. Here we replace the actual random potentials at different sites by an effective,

energy dependent, translationally symmetric potential; such that the Green function corresponding to the effective Hamiltonian is equal to the configuration averaged Green function of the actual system under consideration. By this definition the effective Hamiltonian H_{eff} is related to the configuration averaged Green operator as

$$\langle G(Z)\rangle = (ZI - H_{eff})^{-1} \qquad (2.1.5)$$

From equation (2.1.4) and (2.1.5) it is clear that the constructed effective medium is described by complex energy dependent potentials sitting at various atomic sites. Though the effective medium does not correspond to a real physical system, its Green function is related to the configuration averaged properties of the random system.

Let us illustrate the procedure in a simplified single- band tight-binding model with diagonal disorder. Our Hamiltonian in the tight-binding basis is

$$H = \sum_i \varepsilon_i P_i + \sum_{i\,j} V_{ij}\, T_{ij} \qquad (2.1.6)$$

where i,j are the site indices, P_i and T_{ij} are projection $|i\rangle\langle i|$ and transfer $|i\rangle\langle j|$ operators respectively on the space spanned by the basis $\{|i\rangle\}$. The diagonal or site energies ε_i are random. We take V_{ij} to be some averaged nonrandom value $\langle V_{ij}\rangle$.

Now we define our effective Hamiltonian in the same tight-binding basis as

$$H_{eff} = \sum_i \Sigma_i(E)\ P_i + \sum_{ij} \langle V_{ij} \rangle\ T_{ij}$$

(2.1.7a)

In a single site CPA the self energy $\Sigma_i(E)$ is in general complex and energy dependent. It is also non random and independent of the site index, *i.e.*, $\Sigma_i(E) = \Sigma_o(E)$.

With this our effective Hamiltonian becomes

$$H_{eff} = \Sigma_o(E) \sum_i P_i + \sum_{ij} \langle V_{ij} \rangle\ T_{ij}$$

(2.1.7b)

The only unknown quantity in the calculation of the electron charge density is $\Sigma_o(E)$. The problem is now to determine this self energy or effective medium energy self-consistently, which yields

$$G_{eff}(Z) = \langle\ G(Z)\ \rangle = (ZI - H_{eff})^{-1}\ .$$

(2.1.8)

To do this we consider an exact potential, ε_i which is embedded at the i^{th} site within the effective medium (Figure 2.1) in such a way that no extra scattering is produced on the average.

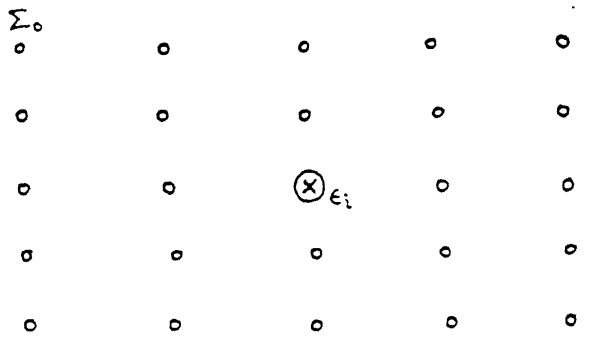

Figure 2.1 :Single potential embedded in an effective medium.

In mathematical language

$$\langle G^i \rangle = G_{eff} = \langle G \rangle$$

(2.1.9a)

where ,

$$G^i = (ZI - H^i_{eff})^{-1}$$

(2.1.9b)

is the Green function for the medium in which all the sites are occupied by $\Sigma_o(E)$ except the site i which is occupied by ε_i. The corresponding Hamiltonian (H^i_{eff}) is

$$H^i_{eff} = H_{eff} + (\varepsilon_i - \Sigma_o) P_i$$

(2.1.10)

Substituting equation (2.1.10) in equation (2.1.9b), it can be written as

$$G^i = \left[ZI - H_{eff} - (\varepsilon_i - \Sigma_o) P_i \right]^{-1}$$

and substituting equation (2.1.8), we obtain

$$G^i = G_{eff} \left[I - \left((\varepsilon_i - \Sigma_o) P_i \right) G_{eff} \right]^{-1}$$

(2.1.11)

Expanding the right hand side of the equation (2.1.11) we get

$$G^i = G_{eff} + G_{eff} \left[(\varepsilon_i - \Sigma_o) P_i \right] G_{eff} \left[I - G_{eff} \left((\varepsilon_i - \Sigma_o) P_i \right) \right]^{-1}$$

$$= G_{eff} + G_{eff} (\varepsilon_i - \Sigma_o) P_i \left[I - G_{eff} (\varepsilon_i - \Sigma_o) P_i \right]^{-1} G_{eff}$$

(2.1.12)

Substituting

$$t_i = (\varepsilon_i - \Sigma_o) P_i \left[1 - G_{eff} \left((\varepsilon_i - \Sigma_o) P_i \right) \right]^{-1}$$

in equation (2.1.12) we obtain

$$G^{(i)} = G_{eff} + G_{eff}\, t_i\, G_{eff}$$

and taking configuration average

$$\langle G^{i} \rangle = G_{eff} + G_{eff} \langle t_i \rangle G_{eff} \qquad (2.1.13)$$

In order to satisfy equation (2.1.9a) we write

$$\langle t_i \rangle = 0 \qquad (2.1.14)$$

Equation (2.1.14) ensures that when an extra potential is embedded in the effective medium there is no extra scattering on the average where t_i describes the scattering.

The self energy $\Sigma_o(E)$ can be obtained from this equation, solving it self-consistently. Here we are interested in studying the electronic properties of binary alloys, for which the i^{th} site either can be occupied by an A atom or a B atom. Therefore, for binary alloys without short-ranged order, equation (2.1.14) reduces to

$$c\,\frac{\varepsilon_A - \Sigma_o}{1-\langle G\rangle(\varepsilon_A - \Sigma_o)} + (1-c)\,\frac{\varepsilon_B - \Sigma_o}{1-\langle G\rangle(\varepsilon_B - \Sigma_o)} = 0 \qquad (2.1.15)$$

where c is the concentration of A atoms in the alloy. *This is the CPA equation for random binary alloy.* To solve this equation self-consistently a suitable initial choice of $G_i(Z)$ is made for $\langle G\rangle$ to start with. We then calculate $\Sigma_o(E)$ from the equation (2.1.15) and then from $\Sigma_o(E)$ we calculate a new $G_i(Z)$. This goes iteratively until $\Sigma_o(E)$ converges. Care must be taken to preserve the Herglotz analytic properties (Mookerjee,1973) related to the physical necessity that the energy spectrum be real and the density of states be positive. This must be preserved at all levels of iterations.

2.2 : A METHOD OF EMBEDDING

The method of Embedding was introduced by Inglesfield (1981) to study the electronic properties of impurities and surfaces. This methodology involves the partition of the space on which the Hamiltonian is defined, into two subspaces I and II with an interface S between them. This is shown in the figure(2.2).

The Hamiltonian for the full space is

$$H = T + V_I + U$$

where V_I and U are the potentials in the subspaces I and II respectively.

If $\Psi(r)$ is the wave function defined for the full space then the Schrödinger equation of the system will be

$$H\ \Psi(r) = E\ \Psi(r) \qquad (2.2.1)$$

where E is the energy eigenvalue.

The advantage here is that the above time independent Schrödinger equation in the full space may be reduced to a Schrödinger equation in the smaller subspace I, through an effective Hamiltonian H^I in subspace I. The effect of the rest of the subspace II, *i.e.*, the complement of I, is incorporated in this effective Hamiltonian as a surface potential, V_s,as shown in figure (2.3).

The effective Hamiltonian (defined in subspace I) is,

$$H^I = T+V_I+V_s \qquad (2.2.2)$$

This surface potential can be constructed from the Green function $G_o(r,r')$ of subspace II which satisfies the usual boundary condition at infinity along with Neumann boundary condition on the surface S,*i.e.*, the normal derivative of the Green function vanishes on the surface S :

$$\frac{\partial}{\partial n_s} G_o(r,r')\Big|_{r,r' \in S} = 0$$

(2.2.3)

To solve the Schrödinger equation in region I we find the expectation value of the energy of the wave function $\Psi(r)$ of the full space, defined in subspace I as a trial wave function $\phi(r)$ and in subspace II as the exact solution of the Schrödinger equation at some energy ε, with the condition that the solutions match correctly on the boundary surface S:

$$(-\tfrac{1}{2}\nabla_r^2 + U(r) - \varepsilon)\psi(r) = 0, \; r \text{ in subspace II}$$

(2.2.4)

and

$$\psi(r_s) = \phi(r_s)$$

(2.2.5)

The expectation value of the Hamiltonian of the full subspace is

$$E = \frac{\int d^3r \; \Psi^*(r) \; H \; \Psi(r)}{\int d^3r \; \Psi^*(r) \; \Psi(r)}$$

(2.2.6)

Substituting equation (2.2.4) in equation (2.2.6) we obtain

$$E = \frac{\int_I d^3r \; \varphi^*(r) H \; \varphi(r) + \varepsilon \int_{II} dr^3 \psi^*(r)\psi(r) + \frac{1}{2}\int d^3r_s \; \varphi^*(r_s)\left[\frac{\partial \varphi(r_s)}{\partial n_s} - \frac{\partial \psi(r_s)}{\partial n_s}\right]}{\int d^3r \; \varphi^*(r)\varphi(r) + \int d^3r \; \psi^*(r)\psi(r)}$$

The final surface integral in the numerator comes from the discontinuity in the derivative between $\phi(r)$ and $\psi(r)$ on the surface S. We now express the normal derivative $\partial\psi(r)/\partial n_s$ across the boundary surface S in terms of $\phi(r_s)$, by using the Green function $G_o(r,r')$ for region II, satisfying the following equation

$$(-\frac{1}{2}\nabla_r^2 + U(r) - \varepsilon)\, G_o(r,r') = \delta(r-r') \tag{2.2.8}$$

where r and r' are in region II.

Multiplying equation (2.2.8) by $\psi(r)$ and equation (2.2.4) by $G_o(r,r')$ and subtracting one from the other we get

$$(-\frac{1}{2}\nabla_r^2\psi(r))G_o(r,r') + (\frac{1}{2}\nabla_r^2 G_o(r,r'))\psi(r) = -\delta(r-r')\psi(r) \tag{2.2.9}$$

Integrating equation (2.2.9) through the region II yields

$$\psi(r) = \frac{1}{2}\int_{II} d^3r'[G_o(r,r')\nabla_{r'}^2\psi(r') - \psi(r')\nabla_{r'}^2 G_o(r,r')] \tag{2.2.10}$$

This integral can be evaluated using Green theorem

$$\int_v [f(r)\nabla_r^2 g(r) - g(r)\nabla_r^2 f(r)]d^3r = \oint_s \left[f(r)\frac{\partial g(r)}{\partial n_s} - g(r)\frac{\partial f(r)}{\partial n_s}\right] dr_s^2$$

where $\partial/\partial n_s$ is the normal derivative at the surface S directed outwards from inside the volume. Using Green theorem the volume integral of equation (2.2.10) reduces to the following surface integral

$$\psi(r) = -\frac{1}{2}\int_s d^2r'_s \left[G_o(r,r'_s) \frac{\partial\psi(r'_s)}{\partial n_s} - \psi(r'_s)\frac{\partial G_o(r,r'_s)}{\partial n_s} \right]$$

(2.2.11)

If we construct G_o to have zero derivative on S, this gives us an equation relating the amplitude of the wave function in II and its normal derivative on S :

$$\psi(r) = -\frac{1}{2}\int_s d^2r'_s\, G_o(r\ ,r'_s)\, \frac{\partial\psi(r'_s)}{\partial n'_s}$$

and putting r on S

$$\psi(r_s) = -\frac{1}{2}\int_s d^2r'_s\, G_o(r_s\ ,r'_s)\, \frac{\partial\psi(r'_s)}{\partial n'_s}$$

(2.2.12)

The inverse of this gives $\partial\psi(r_s)/\partial n_s$ in terms of $\psi(r_s)$,which we have set equal to $\phi(r_s)$, as given by the equation (2.2.13)

$$\frac{\partial\psi(r_s)}{\partial n_s} = -2\int_s d^2r'_s\, \phi(r'_s)\, K(r_s\ ,r'_s)$$

(2.2.13)

where the functional inverse K of G_o is defined by

$$\int K(r,r'')G_o(r'',r')d^3r'' = \delta(r-r')$$

Now to reduce the volume integral $\int_{II} d^3r\ \psi^*(r)\ \psi(r')$ to a surface integral, we vary the energy ε in the equation (2.2.4), but still ensuring that $\psi(r)$ matches with $\phi(r)$, over the interface S, to obtain

$$H\delta\psi(r) = \delta\varepsilon\ \psi(r) + \varepsilon\ \delta\psi(r)$$

Multiplying this and the complex conjugate of equation (2.2.4) respectively by $\psi^*(r)$ and $\delta\psi(r)$ and subtracting one from the other and integrating through subspace II, the above volume integral yields:

$$\int_{II} d^3r\ \psi^*(r)\psi(r) = \frac{1}{2}\int_{II} d^3r\left[\frac{\partial\psi(r)}{\partial\varepsilon}\nabla_r^2\psi^*(r) - \psi^*(r)\nabla_r^2\left[\frac{\partial\psi(r)}{\partial\varepsilon}\right]\right] \qquad (2.2.15)$$

The volume integral on the right hand side can be reduced to the surface integral using Green theorem as follows

$$-\frac{1}{2}\int_s d^2r_s\left[\frac{\partial\psi(r_s)}{\partial\varepsilon}\ \frac{\partial\psi^*(r_s)}{\partial n_s} - \psi^*(r_s)\frac{\partial}{\partial n_s}\left[\frac{\partial\psi(r_s)}{\partial\varepsilon}\right]\right] \qquad (2.2.16)$$

Substituting $\partial\psi(r_s)/\partial n_s$ and it's complex conjugate and using the symmetry of the Green function in the surface integral (2.2.16), the volume integral becomes

$$\int_{II} d^3r\ \Psi^*(r)\Psi(r) = -\int_s d^2r_s \int_s d^2r_s'\ \phi^*(r_s)\frac{\partial}{\partial\varepsilon}\ K(r_s,r_s')\ \phi(r_s') \qquad (2.2.17)$$

Substituting equation (2.2.13) and equation (2.2.17) in equation (2.2.7) we obtain

$$E = \frac{\int_I d^3r\ \varphi^*(r)H\varphi(r) + \frac{1}{2}\int_s d^2r_s\ \varphi^*(r_s)\frac{\partial\varphi(r_s)}{\partial n_s} + \int_s d^2r_s \int_s d^2r'_s\ \phi^*(r_s)\,K(r_s,r'_s)\,\phi(r'_s) - \varepsilon\int_s d^2r_s \int_s d^2r'_s\ \phi^*(r_s)\frac{\partial}{\partial\varepsilon}K(r_s,r'_s)\,\phi(r'_s)}{\int_I d^3r\ \varphi^*(r)\varphi(r) - \int_s d^2r_s \int_s d^2r'_s\ \phi^*(r_s)\frac{\partial}{\partial\varepsilon}K(r_s,r'_s)\,\phi(r'_s)}$$

(2.2.18)

This expression gives E purely in terms of a trial wave function $\phi(r)$ defined in the subspace I and in the interface S. Now the variational minimization of E with respect to the trial wave function $\phi^*(r)$, *i.e.*, $\delta E/\delta\phi^*(r)=0$, gives the effective Schrödinger equation. If we evaluate the Green function at the eigenvalues $\varepsilon = E$ on the spectrum, this effective Schrödinger equation reduces to

$$-\frac{1}{2}\nabla_r^2\phi(r) + \frac{1}{2}\,\delta(n-n_s)\,\frac{\partial\varphi(r)}{\partial n_s} + v(r)\phi(r) + \delta(n-n_s)\int_S d^2r'_s\ K(r_s,r'_s,E)\,\phi(r'_s) = E\,\phi(r)$$

with r in subspace I.

(2.2.19)

This effective Schrödinger equation acts only on subspace I and the effect of the subspace II appears as a surface potential

operator $\delta(n-n_s)\int_s d^2r'\ K(r_s,r_s',E)$. The term $(1/2)\delta(n-n_s)(\partial/\partial n_s)$ ensures that the effective Hamiltonian remains Hermitian in region I alone. Usually region I is a small subspace of the Hilbert space, so that equation (2.2.19) is a significant simplification, provided that we can determine the surface potential $K(r_s, r_s', E)$ on the surface with ease.

2.2.1: THE CALCULATIONAL PROCEDURE

For actual calculations of the resolvant operator,we need a representation of the effective Hamiltonian (in subspace I) in a suitably chosen basis. To obtain this we expand the trial wave function in subspace I in terms of countable basis functions $\chi_m(r)$ which span subspace I and reflect the symmetry of the solution we wish to study

$$\phi(r) = \sum_m a_m \chi_m(r) \qquad (2.2.20)$$

Using this basis and minimizing energy E with respect to the variational parameter a_m, we obtain the matrix representation of the effective Schrödinger equation (2.2.19):

$$\sum_m H_{nm}\, a_m = E \sum_m O_{nm}\, a_m \qquad (2.2.21)$$

The effective Hamiltonian matrix is

$$H_{nm} = \int_I d^3r\ \chi_n(r)\left[-\tfrac{1}{2}\nabla_r^2 + V(r)\right]\chi_m(r) + \tfrac{1}{2}\int_s d^2r_s\ \chi_n(r_s)\frac{\partial \chi_m(r_s)}{\partial n_s}$$

$$+\int_s d^2r_s \int_s d^2r_s' \chi_n(r_s) K(r_s, r_s', E) \chi_m(r_s')$$

(2.2.22a)

and the overlap matrix is

$$O_{nm} = \int_I d^3r \chi_n(r) \chi_m(r)$$

(2.2.22b)

2.3: CPA THROUGH EMBEDDING

We shall now develop CPA through this Embedding technique. The effective medium is described by an effective unknown potential term. This can be constructed from the Green function $G_o(r,r',E,U)$ where U is the coherent potential of subspace II, to be determined self-consistently.

Before going on to develop the CPA through embedding let us review the philosophy which underlines the CPA as well as the Embedding method.

Inglesfield's idea is based on the fact that the solutions of the second order elliptic differential equations (such as Schrödinger equation) in all space may be solved by confining ourselves to a small finite closed subspace. The effect of the remaining space is incorporated in the effective Hamiltonian as a surface potential.

In the single site CPA we find the self energy or effective medium energy self-consistently by embedding an exact potential ε_i at the i^{th} site within the effective medium in such a way that no extra scattering is produced on the average. In mathematical language this is

$$\langle G^I(V_I, U)\rangle_{(V_I)} = G_{eff}(U) \qquad (2.3.1)$$

where $G_{eff}(U)$ is the Green function of the effective medium and the averaged Green function in equation (2.3.1) is averaged over different configurations of V_I in subspace I alone.

Preserving the essence of these approaches we now develop our new , Embedding-CPA formalism in the following steps:

We divide the space into two subspaces I and II with an interface S. In subspace I we take the potential $V(r)=V_I(r)$ exactly as a random potential whereas in subspace II the potential U(r) is replaced by an effective energy dependent non-random, translationally symmetric coherent potential $U_{coh}(r,E)$: $U_{coh}(r+R,E) = U_{coh}(r,E)$, where R is lattice translation vector.

As described in CPA, coherent potential or self energy is obtained, embedding a small region of the exact potential $V_I(r)$ with a particular configuration in this effective medium *(region II)* so that no extra scattering is produced on the average :

$$\langle G(r,r',V,U,E)\rangle = G_{eff}(r,r',U,E) \qquad (2.3.2)$$

where $G(r,r',V,U,E)$ is the embedding Green function of subspace I satisfying the effective Schrödinger equation:

$$(H^I - EI)\, G(r,r',V,U,E) = \delta(r-r'),$$

H^I is the corresponding effective Hamiltonian.

The effective medium Green function $G_{eff}(r,r',U,E)$ is obtained from a Hamiltonian where the Coherent Potential $U(r,E)$ is substituted for the entire space. Equation (2.3.2) reflects CPA in a more general way without considering a particular basis in region I.

2.3.1: CALCULATION OF EMBEDDED GREEN FUNCTION

First let us construct the embedded Green function which is needed to study the electronic properties of a disordered system applying Embedding-CPA method. This Green function satisfies the following equation:

$$-\frac{1}{2}\nabla_r^2 G(r,r',U,E) + \frac{1}{2}\delta(n-n_s)\frac{\partial}{\partial n_s} G(r,r',U,E)$$

$$+ (V(r)-E)\, G(r,r'.U,E)$$

$$+\delta(n-n_s)\int_S d^2r_s''\, K(r_s,r_s'',U,E)\, G(r_s'',r',U,E) = \delta(r-r')$$

where r,r'are in subspace I.

(2.3.3)

Let us take a representation of equation (2.3.3) in a basis $\{\chi_n(r)\}$ which spans subspace I and which is suitably chosen to reflect any symmetry of the solution required. Expanding the Green function in terms of this set of basis functions:

$$G(r,r') = \sum_{nm} G_{nm}\, \chi(r)\, \chi(r')$$

and substituting in equation (2.3.3) we obtain

$$G(r,r') = \sum_{nm} G_{nm}\Big[-\tfrac{1}{2}\nabla_r^2\, \chi_n(r) + \tfrac{1}{2}\,\delta(n-n_s)\,\frac{\partial}{\partial n_s}\chi_n(r_s) + V(r)\chi_n(r)$$

$$+ \delta(n-n_s)\int_S d^2r_s''\, K(r_s,r_s'',U_{coh},E)\chi_n(r_s'') - E\chi_n(r)\Big]\chi_m(r') = \delta(r-r').$$

(2.3.4)

Multiplying this by $\chi_k^*(r)\chi_l^*(r')$ and integrating over r and r' through the region I we obtain

$$\sum_{nm} (H_{kn} - E\, O_{kn})\, G_{nm}\, O_{ml} = O_{kl}$$

(2.3.5)

where the Hamiltonian and overlap matrix elements are given by equation (2.2.22a) and equation (2.2.22b) respectively. Linear independence of basis then yields

$$\sum_k (H_{nk} - EO_{nk})\, G_{km} = \delta_{nm}$$

(2.3.6)

So the matrix representation of the embedded Green function is the following resolvant matrix :

$$G_{nm} = (H-EO)^{-1}_{nm}\ .$$

In the continuum range of energy it is useful to work with the local density of states n(r,E), that is, the charge density of electrons with energy E. This can be directly found from the imaginary part of the embedded Green function:

$$n(r,E) = \frac{1}{\pi} \sum_{nm} \mathrm{Im}\left[(H-EO)^{-1}_{nm}\right] \chi_n(r)\, \chi_m(r), \quad r \text{ in subspace I}$$

(2.3.7a)

The total density of states is related to the above through

$$n(E) = \int_I d^3r\, n(r,E)$$

(2.3.7b)

and the charge density is

$$\rho(r) = e \int_{-\infty}^{\mu} dE\, n(r,E)$$

(2.3.7c)

where μ is the chemical potential. The number density of electrons is given by

$$n = \int_{-\infty}^{\mu} dE\, n(E) \ .$$

(2.3.7d)

2.3.2: CALCULATION OF THE EFFECTIVE MEDIUM GREEN FUNCTION

We shall illustrate our formalism by applying it to a simple example. Here region I is a sphere of radius r_s centred at the origin with a random single muffin -tin potential $V_I(r)$. The boundary is a spherical interface S, as shown in the figure(2.4).

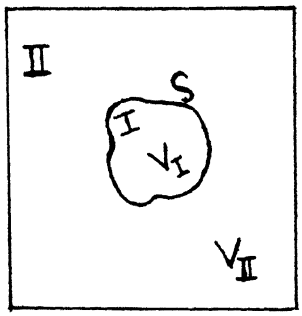

Figure 2.2 : Partition of space into two subspaces.

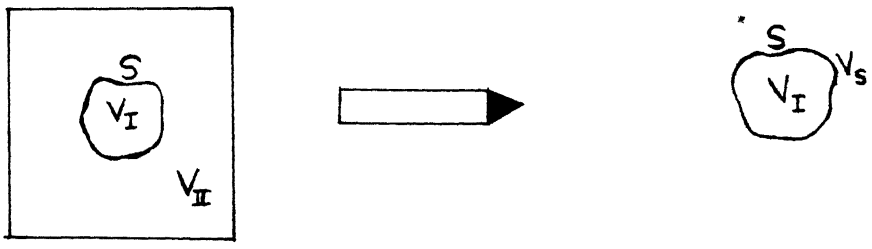

Figure 2.3 : Advantage of embedding formalism.

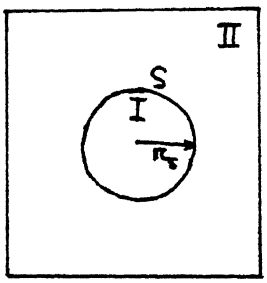

Figure 2.4 : Muffin-tin potential embedded in region II.

For simplicity of calculation, we take a Coherent Jellium in region II. This assumes that the Coherent potential is independent of r but strongly energy dependent : $U(r,E) = U(E)$

The Green function $G_o(r,r',E,U)$ can be expanded as

$$G_o(r,r',U,E) = -i\varkappa \sum_L \left[j_l(\varkappa r_<) - \frac{j_l'(\varkappa r_s)}{h_l'(\varkappa r_s)} h_l(\varkappa r_<) \right] h_l(\varkappa r_<) \; Y_L(\hat{r}) Y_L(\hat{r}') \qquad (2.3.8)$$

where j_l are spherical Bessel functions, h_l are Hankel functions and $Y_L(\hat{r})$ are spherical harmonics and $\varkappa$ is defined as $[2(U(E) - E)]^{1/2}$. Here L and $\hat{r}$ denote the angular momenta unit vector in the direction of r, described by the angular variables (l,m) and (θ,ϕ) respectively.

On the boundary surface S this Green function becomes

$$G_o(r_s, r_s', U, E) = -i\varkappa \sum_L W(j_l,h_l) \frac{h_l(\varkappa r_s)}{h_l'(\varkappa r_s)} Y_L(\hat{r}) Y_L(\hat{r}')$$

$$= \sum_L g_l(\varkappa r_s) Y_L(\hat{r}) Y_L(\hat{r}') \qquad (2.3.9)$$

where

$$g_l(\varkappa r_s) = -i\varkappa \, W(j_l,h_l) \left[\frac{h_l(\varkappa r_s)}{h_l'(\varkappa r_s)} \right] \qquad (2.3.10)$$

and the Wronskian is

$$W(j_l,h_l) = j_l(\varkappa r_<)h_l'(\varkappa r_s) - j_l'(\varkappa r_s)h_l(\varkappa r_<)$$

This g_l is related to its functional inverse as

$$r_s^4\, k_l(\varkappa r_s)g_l(\varkappa r_s) = 1 \qquad (2.3.11)$$

Substituting equation (2.3.10) in equation (2.3.11) we get

$$k_l(\varkappa r_s) = \frac{i}{\varkappa\, r_s^4}\ \frac{1}{W(j_l,h_l)}\left[\frac{h_l'(\varkappa r_s)}{h_l(\varkappa r_s)}\right] \qquad (2.3.12)$$

and

$$K(r_s, r_s', U, E) = \sum_L k_l(\varkappa r_s)Y_L(\hat{r})Y_L(\hat{r}') \qquad (2.3.13)$$

Here the $\varkappa$ dependence of the surface potential shows that the effective Hamiltonian or embedded Green function depends upon the coherent potential of subspace II.

CHAPTER III

COHERENT JELLIUM MODELS

In this chapter we shall illustrate our Embedding-CPA formalism by simple examples. We take examples of random binary alloys, $A_c B_{1-c}$ where c is the concentration of A type of atoms in the alloy. $V_I(r)$ is the binary alloy potential in region I. In region II, we take a Coherent Jellium potential, *i.e.*, a potential that is independent of the spatial variable r, but depends only on energy E : $U(r,E) = U(E)$. In this model the lattice effects are suppressed. Such models are appropriate in cases where long range lattice ordering is absent, as in liquid alloys.

3.1: ELECTRONS WITH S-SYMMETRY IN SQUARE WELL POTENTIAL

We shall study the s wave local density of states in flat potentials, *i.e.*, the potentials $V_I(r) = V_A$ or V_B in region I and zero outside. In this subspace I we choose our basis function to be

$$\chi_m(r) = \frac{\sin mr}{r} \qquad (3.1.1)$$

In this basis the surface potential from equation (2.3.13) can be written as:

$$K(r_s,r_s',U_{coh},E) = \frac{1}{\varkappa r_s^4}\,\frac{1}{W(j_l,h_l)}\left[\frac{h_o'(\varkappa r_s)}{h_o(\varkappa r_s)}\right] Y_{oo}(\hat{r})\, Y_{oo}(\hat{r}') \qquad (3.1.2)$$

where, $\varkappa = \left[\, 2(\, U(E)-E\,)\,\right]^{1/2}$ and $L = (l,m) = (0,0)$.

Substituting the Hänkel function, $h_o(x) = -(1/ix)\exp(-ix)$ and Bessel function $j_o(x) = \frac{\sin x}{x}$, where $x = \varkappa r$, we obtain

$$K(r_s,r_s',U,E) = \left[\frac{1-i\varkappa r_s}{2r_s^3}\right] Y_{oo}(\hat{r})\, Y_{oo}(\hat{r}') \qquad (3.1.3)$$

Now, in the given basis and with this surface potential, the effective Hamiltonian matrix element is given by

$$H_{nm} = \left[\frac{1}{2}\,n^2 + V_I(r)\right] O_{nm} + \frac{1}{2}\sin nr_s\left[m\cos mr_s - \left(\frac{\sin mr_s}{r_s}\right)\right] + \sin nr_s \sin mr_s \left[\frac{1-i\varkappa r_s}{2r_s}\right] \qquad (3.1.4)$$

where the overlap matrix O_{nm} is given as

$$O_{nm} = \frac{1}{2}\left[\frac{\sin(n-m)r_s}{(n-m)} - \frac{\sin(n+m)r_s}{(n+m)}\right]$$

(3.1.5a)

For a single member basis function, i.e., when m = n, the above matrix element will become

$$H_{nn} = \left[\left(\frac{1}{2}n^2 + V_I(r)\right) O_{nn} + \frac{n}{4}\sin 2nr_s\right] - \frac{i\varkappa \sin^2 nr_s}{2}$$

and

$$O_{nn} = \frac{1}{2}\left[r_s - \frac{\sin 2nr_s}{2n}\right]$$

(3.1.5b)

The unknown $\varkappa$ in H_{nn} can be obtained from CPA equation given by

$$c\, G_{nn}(V_A, U, E) + (1-c)\, G_{nn}(V_B, U, E) = G_{nn}(E, U).$$

(3.1.6)

Equivalently this can also be reduced to

$$\left[\frac{iB_{nn}O_{nn}}{2}\right]\varkappa^3 + \left[\frac{A_{nn}O_{nn} - \tilde{V}O^2_{nn}}{2}\right]\varkappa^2 - iB_{nn}O_{nn}\,\bar{(E+V)}\,\varkappa + \left[(V_A V_B + E\tilde{V})\,O^2_{nn} - A_{nn}(\tilde{V}+E)\right] = 0$$

(3.1.7a)

where we have used the following relations :

$$\bar{V} = c\,V_A + (1-c)\,V_B$$

$$\tilde{V} = (1-c)\,V_A + c\,V_B$$

$$A_{nn} = \frac{1}{2}\,O_{nn} + \frac{n}{4}\sin 2nr_s - E\,O_{nn}$$

$$B_{nn} = \frac{1}{4}(\cos 2nr_s - 1)$$

$$U_{coh}(E) = (\frac{\varkappa^2}{2} + E)$$

(3.1.7b)

Equation(3.1.7a) is a cubic order polynomial equation in $\varkappa$. We calculate the density of states for all these complex roots of the polynomial. The negative density of states with Herglotz analytic properties is the correct choice of the density of states.

3.1.1: RESULTS

Figure 3.1(a) shows the density of states for V_A = -1.0 au and V_B = -5.0 au ,r_s = 2 au ,c = 0.5. The broken curve is obtained for n = 1 and the full curve for n = 8.The essential qualitative features are already reproduced for n = 1, whereas increasing n leads to shifts in the peaks as well as in the broadening. Essential differences occur at higher energies. Figure 3.1(b) shows the result for the same potentials but for concentration c = 0.9 at higher energy regimes for n = 4 (broken curve) and n = 8 (full curve). The two differ very little except at very high energies and even then the ratio of the difference to the average peak height is only about 4%.

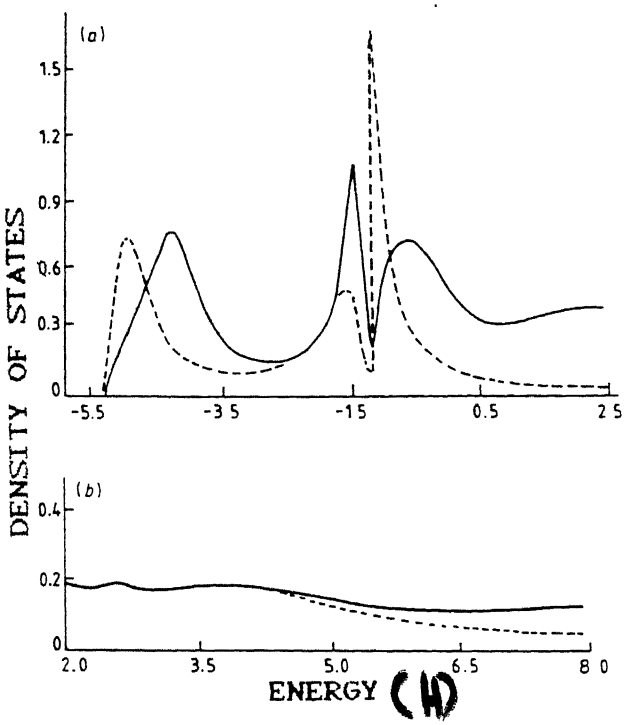

Figure 3.1 : (a) Densities of states for V_A=-1.0 au, V_B=-5.0au, r_s=2 au and c=0.5: ---, single member basis; ——, eight member basis. (b) Difference in the densities of states for a four member basis(---)calculation and an eight member basis calculation(——)for the same parameters as above with c=0.9 at higher energies.

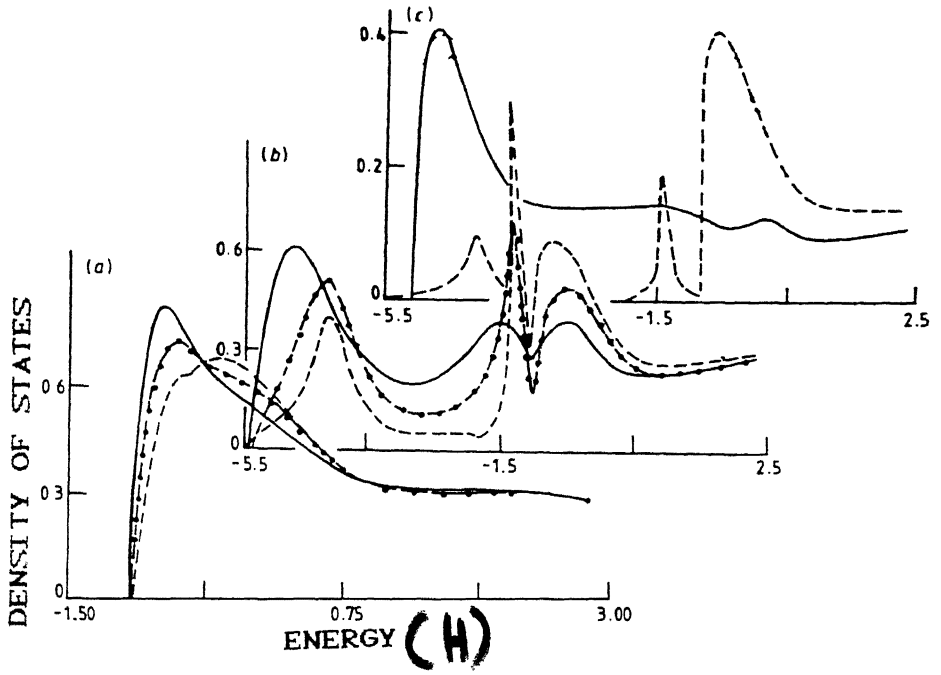

Figure 3.2 : Densities of states for s states in flat potential binary alloy with (a) V_A=-0.5 au and V_B=-1.0 au, (b) V_A=-1.0 au and V_B=-5.0 au and (c) V_B=-5.0 au and V_A=-0.5 au. For (a) and (b): (- - -) c=0.3; (- · -) c=0.5; (——) c=0.7; for (c): (- - -) c=0.1; —— c =0.9.

To illustrate the effect of the concentration and $|V_A - V_B|$ (the two parameters characterising disordered alloys), we show in figure 3.2 three sets of alloys for n = 1 (broken curves) and n = 8 (full curves) and c = 0.3, 0.5, 0.7.

Figure 3.2(a) is for V_B = -1.0 au and V_A = -1.0 au. This is the overlapping-band weak disorder case. The peaks corresponding to the constituents overlap to form a broad structure; the relative weights of each constituent are reflected in the concentration.

Figure 3.2(b) is for V_B = -5.0 au and V_A = -1.0 au. This is the *split-band* strong-scattering regime. Each constituent contributes distinguishable structures whose weights again are reflected in the concentrations.

Figure 3.2(c) is for V_B = -5.0 au and V_A = -0.5 au and c = 0.1 and 0.9. This is the so called *impurity-band* strong-scattering regime. It is here that, from our experience with tight-binding calculations, cluster effects (not reflected in the CPA calculation here) are expected to dominate.

3.2: ELECTRON WITH D-SYMMETRY IN SQUARE WELL POTENTIAL

Now we shall look at the density of states for d-like states in a flat potential. Our basis function is then:

$$\chi_m(r) = \left[\left(3/mr^3 - 1/mr \right) \sin mr - \left(3/mr^2 \right) \cos mr \right] Y_{22}(\hat{r})$$

(3.2.1)

The surface potential in this case will be

$$K(r_s, r_s', U, E) = (1/2\ r_s^3) \left[\frac{-i\varkappa^3 r_s^3 - 4\varkappa^2 r_s^2 - 9i\varkappa r_s + 9}{-\varkappa^2 r_s^2 - 3i\varkappa r_s + 3} \right] Y_{22}(\hat{r})\ Y_{22}(\hat{r}')$$

(3.2.2)

where we have taken the following Hänkel function

$$h_2(x) = i \left[\frac{1}{x} + \frac{3i}{x^2} - \frac{3}{x^3} \right] e^{ix}$$

and the Bessel function is

$$j_2(x) = \left[\frac{3}{x^3} - \frac{1}{x} \right] \sin x - \frac{3}{x^2} \cos x$$

with $x = \varkappa r$.

Here the effective Hamiltonian matrix for a single member basis with $m = n$ is

$$H_{nn} = (1/2\ n^2 + V_I(r)\ )\ O_{nn} + C_{nn} + B_{nn}\ \varkappa'$$

(3.2.3)

where the overlap matrix is

$$O_{nn} = \left[\frac{1}{2n^2} \left(r_s - \frac{\sin 2nr_s}{2n} \right) + \frac{3}{2} \frac{\cos 2nr_s}{n^6 r_s^3} - \frac{3}{2} \frac{\cos 2nr_s}{n^4 r_s} \right.$$

$$\left. - \frac{3\sin 2nr_s}{n^6 r_s^2} - \frac{3}{2n^4 r_s} - \frac{3}{2n^6 r_s^3} \right]$$

(3.2.4)

$$C_{nn} = \frac{1}{2}\left[\left(-\frac{27}{n^6 r_s^5}+\frac{3}{n^4 r_s^3}+\frac{2}{n^2 r_s}\right)\sin^2 nr_s + \left(\frac{54}{n^9 r_s^4}-\frac{6}{n^3 r_s^2}+\frac{1}{n}\right)\cos nr_s \sin nr_s - \left(-\frac{9}{n^4 r_s^3}-\frac{3}{nr_s}\right)\cos^2 nr_s\right]$$

$$B_{nn} = \frac{1}{2}\left[\left(\frac{9}{n^6 r_s^5}-\frac{6}{n^4 r_s^3}+\frac{1}{n^2 r_s}\right)\sin^2 nr_s - \left(\frac{27}{n^5 r_s^4}+\frac{6}{n^3 r_s^2}\right)\cos nr_s \sin nr_s + \left(\frac{9}{n^4 r_s^3}\right)\cos^2 nr_s\right]$$

and $$\varkappa' = \left[\frac{-i\varkappa^3 r_s^3 - 4\varkappa^2 r_s^2 - 9i\varkappa r_s + 9}{-\varkappa^2 r_s^2 - 3i\varkappa r_s + 3}\right]$$

Here CPA equation reduces to the following 5th order polynomial equation in $\varkappa$.

$$\frac{iB_{nn} r_s^3}{2}\varkappa^5 + \left(\frac{A_{nn} r_s^2}{2} - \frac{\tilde{V} O_{nn} r_s^2}{2} - 2r_s^2 B_{nn}\right)\varkappa^4 + \left(\frac{3ir_s A_{nn}}{2} - \frac{3ir_s \tilde{V} O_{nn}}{2} - \frac{9ir_s B_{nn}}{2} - ir_s^3 B_{nn} E - i\bar{V} B_{nn} r_s^3\right)\varkappa^3$$

$$-\Big[\ EA_{nn}r_s^2 + \frac{3A_{nn}}{2} - \frac{3\tilde{V}\,O_{nn}}{2} - \tilde{V}\,O_{nn}r_s^2\,E - \frac{9B_{nn}}{2} - 4B_{nn}r_s^2\,E + A_{nn}\tilde{V}r_s^2$$

$$-V_A V_B\,O_{nn}r_s^2 - 4r_s^2 B_{nn}\bar{V}\ \Big]\ \varkappa^2$$

$$-\Big[3iEA_{nn}r_s + 3ir_s E\,\tilde{V}\,O_{nn} - 9ir_s B_{nn}E + 3iA_{nn}\tilde{V}r_s - 3ir_s V_B V_A O_{nn}$$

$$-9ir_s\tilde{V}B_{nn}\ \Big]\ \varkappa$$

$$+\ \Big[3EA_{nn} - 3\tilde{V}O_{nn}E - 9B_{nn}E - 3V_A V_B O_{nn} + 3A_{nn}\tilde{V} - 9B_{nn}\bar{V}\ \Big] = 0$$

(3.2.5)

where $A_{nn} = \left[\frac{n^2}{2} - E\right] O_{nn} + C_{nn}$. $\tilde{V}$ and $\bar{V}$ are as given in equation (3.1.7b).The correct choice of density of states can be obtained according to the criterion given in section 3.1.

3.2.1: RESULTS

Figures 3.3 (a)-(c) shows the d-state density of states for the corresponding parameters of the s-states shown in the earlier figures. The structures are sharper. This is to be expected since the d-states fall away more sharply from the well centres than do the s-states. The qualitative features are well reproduced by the single member basis.

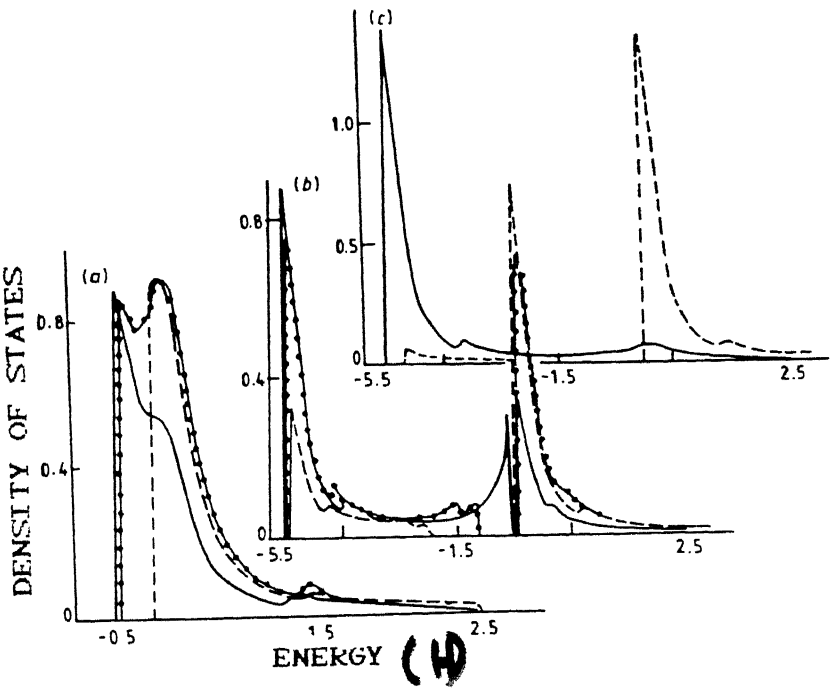

Figure 3.3 : Densities of states for the d states in a flat potential binary alloy with the same parameters as the corresponding parts in figure 3.2.

3.3: ELECTRONS WITH S-SYMMETRY IN HYDROGEN LIKE POTENTIAL

To study effect of the well shape, we next carry out a similar calculation for a 1/r type of potential. We shall look at the s like states in the 1/r type of potential :$V_I(r)=(V_I)/r$ where $V = V_A$ or V_B . The basis function is

$$\chi_m(r) = 2m^{3/2} \exp(-mr)\, Y_{oo}(\hat{r}).$$

Though the shape of the potential is different but it still retains the s symmetry in its lowest energy state. Here the surface potential will be same as given by expression (3.1.9).

In a single member basis, i.e., the overlap matrix will be

$$O_{nn} = 4n^3 \left[\exp(-2nr_s)\left(\frac{-nr_s^2}{2} - \frac{n^2 r_s}{2} - \frac{n^3}{4} \right) + \frac{n^3}{4} \right]$$

and the effective Hamiltonian matrix will be

$$H_{nn} = -\frac{n^2}{2} O_{nn} + (n + V_I)\, C_{nn} + D_{nn} - i\alpha\, B_{nn} \qquad (3.3.1)$$

where $B_{nn} = 2\, n^3\, r_s^2 \exp(-2nr_s)$

$$C_{nn} = 4n^3 \left[\exp(-2nr_s)\left(-\frac{nr_s}{2} - \frac{n^2}{4} \right) + \frac{n^2}{4} \right]$$

$$D_{nn} = (2n^3 r_s - 2n^4 r_s^2)\exp(-2nr_s)$$

Now the Fock-Dirac-CPA equation will be

$$\frac{i\,B_{nn}\,O_{nn}}{2}\,\varkappa^3 + \left[\frac{1}{2}\,\tilde{V}\,C_{nn}O_{nn} - \frac{1}{2}\,O_{nn}A_{nn}\right]\varkappa^2 - iB_{nn}C_{nn}(E+\bar{V})\,\varkappa$$

$$+ (E\,C_{nn}\,A_{nn} - \tilde{V}E\,C_{nn}^2 + \bar{V}C_{nn}\,A_{nn} - V_A V_B C_{nn}^2) = 0 \qquad (3.3.2)$$

and

$$A_{nn} = [\,n^3 r_s - 2n^4\,r_s^2\,]\exp(-2nr_s)$$

Here also we have used the set of relations given in equation (3.1.7b). This is again a cubic order polynomial in $\varkappa$ and the choice of the root is the same as before. Once we get the root,the calculation of local density of state follows the same procedure as described in previous cases.

3.3.1: RESULTS

Figure 3.4 shows the effect of the well shape. We have taken the two potentials to be $V_I(r) = (V_I)/r$ where V can be either V_B or V_A. The qualitative features remain unchanged from the flat potentials,although the quantitative change in the location and the widths of the structures are apparent. The structures are sharper than the flat potentials, which is a reflection of the fact that the flat well s states fall off as 1/r, whereas the 1/r potential wavefunction decays exponentially. The density of states also correspondingly decay at higher energies, and the peak widths are narrower.

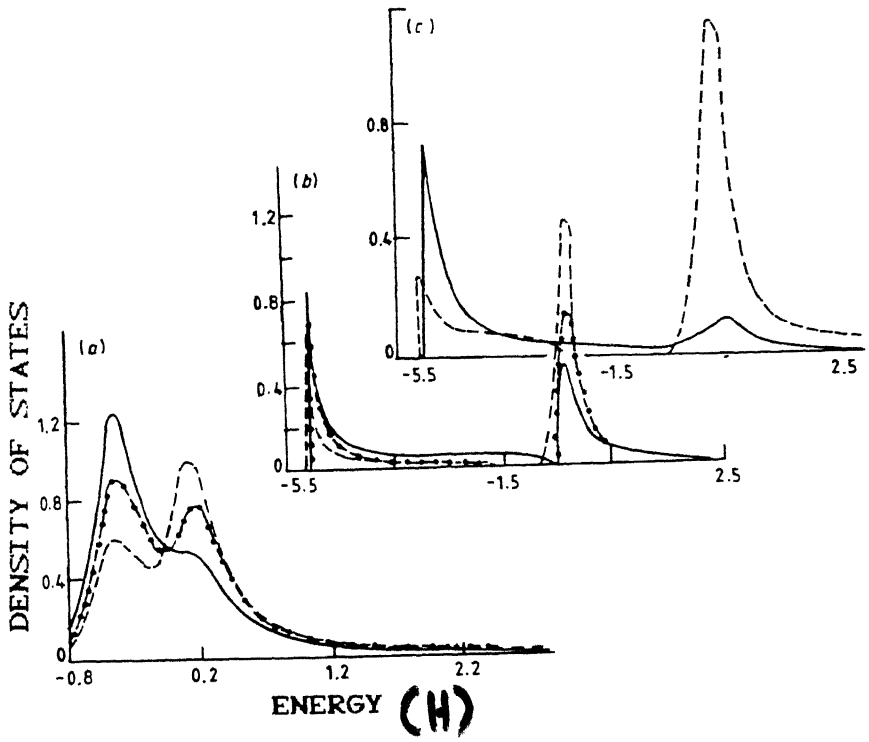

Figure 3.4 : Densities of states for the s states in a binary alloy with potentials of the form V(r)=V/r, with V taking the values V_A and V_B with probabilities c and (1-c). The parameters are the same as in the corresponding parts in figure 3.2 and 3.3.

3.4: ELECTRONS IN NON-SPHERICAL POTENTIAL

In the previous discussion, we have examined several model cases embedding spherically symmetric potential in Coherent Jellium. In this section we study single sites and we extend the idea of the Embedding method to non-spherical potentials and study the effect of non-sphericity in the Coherent Jellium model. Here we consider the potential in subspace I to be of the form

$$V_I(r) = (-V_I/r + \lambda\, r \cos\vartheta) \tag{3.4.1}$$

where the equipotential surfaces are ellipses, figure(3.6). Here λ measures the deviation from sphericity, V_I can take the values V_B or V_A with probabilities c and (1-c) respectively for a binary distribution of the alloy. For small values of λ the chosen basis will be (Luban & Nudbr-Blum 1977)

$$\chi(r) = 2.\exp(-r)\left[1.- \lambda\,(r+1/2\, r^2)\, Y_{10}(\vartheta,\phi)\right] \tag{3.4.2}$$

The effective Hamiltonian matrix in this single member basis, *i.e.*, with n = 1 is given by

$$H_{nn} = A_{nn} - V_I\, C_{nn} - i\,\varkappa'\, B_{nn} \tag{3.4.3}$$

where $$A_{nn} = 2\pi^{-1/3}\left[I_1 - 4/3\, I_4 - 2/3\, I_5 - 1/2\, I_2 + r_s \exp(-2r_s)\right]$$

$$B_{nn} = 2\pi^{-1/3} \exp(-2r_s)$$

$$C_{nn} = 2\pi^{-1/3}\left[4/3\ \lambda^2\left\{I_3+I_4+1/4\ I_5\right\} - I_1\right]$$

$$\varkappa' = \frac{-3i\varkappa r_s - 2\varkappa^2 r_s^3 + r_s}{1 - i\varkappa r_s}$$

and $$I_n = -1/2\ r_s^n \exp(-2r_s) + n/2\ I_{n-1} \quad ,n > 2$$

(3.4.4)

and $$I_1 = -1/2\ r_s \exp(-2r_s) - 1/4 \exp(-2r_s) + 1/4$$

The overlap matrix is given by

$$O_{nn} = -4/3\ \pi^{-1/3}\left[I_2 + I_4 + 1/4\ I_6 + I_5\right]$$

The surface potential will be

$$K(r_s,r_s',U,E) = \left(\frac{1-i\varkappa r_s}{2r_s^3}\right) Y_{00}(\hat{r})\ Y_{00}(\hat{r}')$$

$$+\frac{1}{2r_s^3}\left(\frac{1-2i\ \varkappa r_s - \varkappa^2 r_s^2}{1-i\ \varkappa r_s}\right) Y_{10}(\hat{r})\ Y_{10}(\hat{r}').$$

(3.4.5)

Here we have used the following Bessel and Hänkel functions

$$j_o(x) = \frac{\sin x}{x} \quad ; \quad h_o(x) = \frac{1}{ix}\exp(ix)$$

$$j_1(x)= \frac{\sin x}{x^2} - \frac{\cos x}{x} \quad ; \quad h_1(x)= - \frac{1}{x}\left(1+ \frac{i}{x}\right) \exp(ix)$$

and α can be calculated from the CPA equation which reduces to the following fourth order polynomial equation in α.

$$(-iB_{nn}C_{nn}r_s^3)\alpha^4 + \tfrac{1}{2}(3B_{nn}C_{nn}r_s^3 - ir_s EO_{nn}C_{nn} + ir_s C_{nn}A_{nn} - ir_s C_{nn}^2 \tilde{V})\alpha^3$$

$$+\tfrac{1}{2}(EO_{nn}C_{nn} - C_{nn}A_{nn} + C_{nn}\tilde{V} + 4iB_{nn}C_{nn}Er_s^3 + 4iB_{nn}C_{nn}\bar{V}r_s^3)\alpha^2$$

$$+(iE^2O_{nn}C_{nn}r_s - iEC_{nn}A_{nn}r_s + iEC_{nn}^2\tilde{V}r_s - 3B_{nn}C_{nn}Er_s^2 - iEO_{nn}C_{nn}\bar{V}r_s + iC_{nn}A_{nn}\bar{V}r_s$$

$$-iV_A V_B C_{nn}^2 r_s + 3B_{nn}C_{nn}\bar{V}r_s^2)\alpha$$

$$+(2iBC\bar{V}r_s - E^2OC - ECA - C^2\bar{V}E - iBCEr_s - EOC\bar{V} + CA\bar{V} - V_A V_B C^2) = 0$$

(3.4.6)

3.4.1: RESULTS

In this calculation $V_I = V_A$ or V_B with probability c and 1-c in the region I with λ = .2, .5 and .8 respectivly.

Figure 3.5(a) shows density of states for V_A= -.5au,V_B = -1.au ,c=.5 and with the above given values of λ. This is the overlapping- band weak- disorder case. The peaks corresponding to the constituents overlap to form a broad structure. As the

deviation from sphericity increases overlap increases and the peaks are shifted to the lower energy side.

Figure 3.5 (b) shows a result for V_A = 5. au, V_B= 1. au and c = .5 with the above values of λ. This is the split-band strong band, strong scattering case. Here the peaks become wider and are shifted towards the low energy. This effect is particularly prominent for low energy peaks.

Figure 3.5(c) shows a result for V_A = 5. au , V_B= 1. au and c = .1 where the values are same as taken above. This is the impurity band strong scattering region. Here the more prominent effect of non-sphericity shows up in the lower energy impurity band.

These results are to be compared to the spherical potentials case for the parameter shown in figure 3.4.

Figure 3.6 shows non-spherical equipotential surfaces.

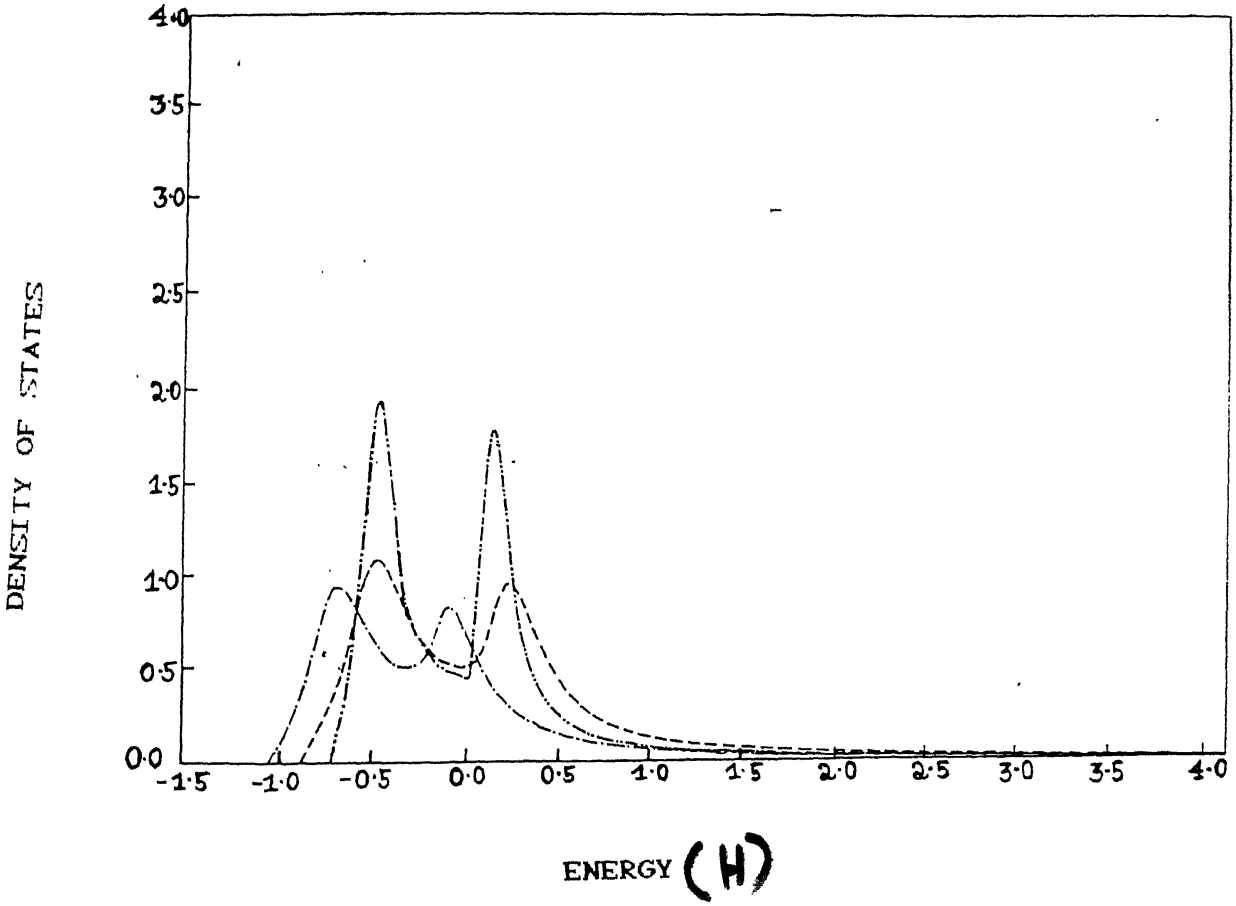

Figure 3.5 :(a) Densities of states for V_A =-0.5 au, V_B =-1.0 au, c=0.5, r_s =2.au ;--- for λ = 0.5;-•- for λ=.8,-. . - for λ= 0.2.

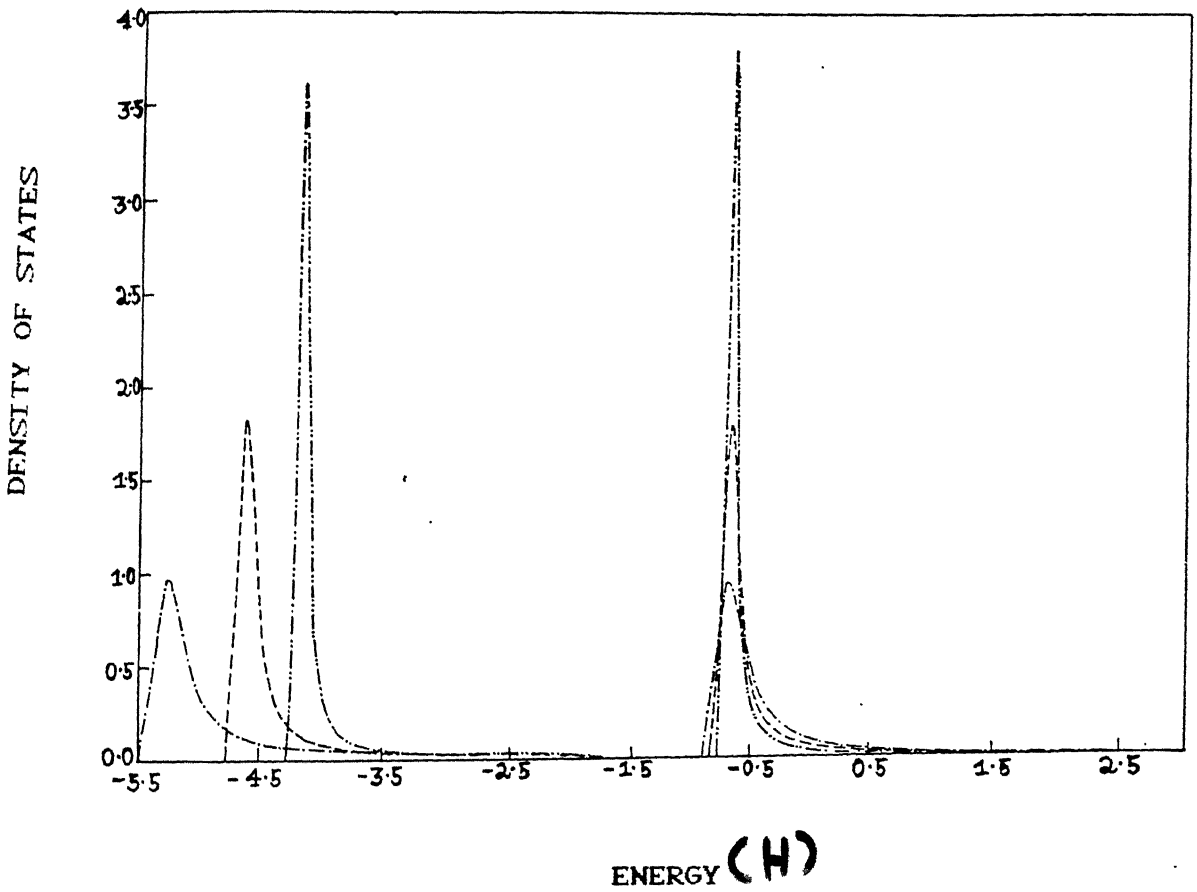

Figure 3.5 :(b) Densities of ststes for V_A = 5.0 au, V_B=1.0 au, c=0.5 with the same λ'S as given in figure 3.1(a).

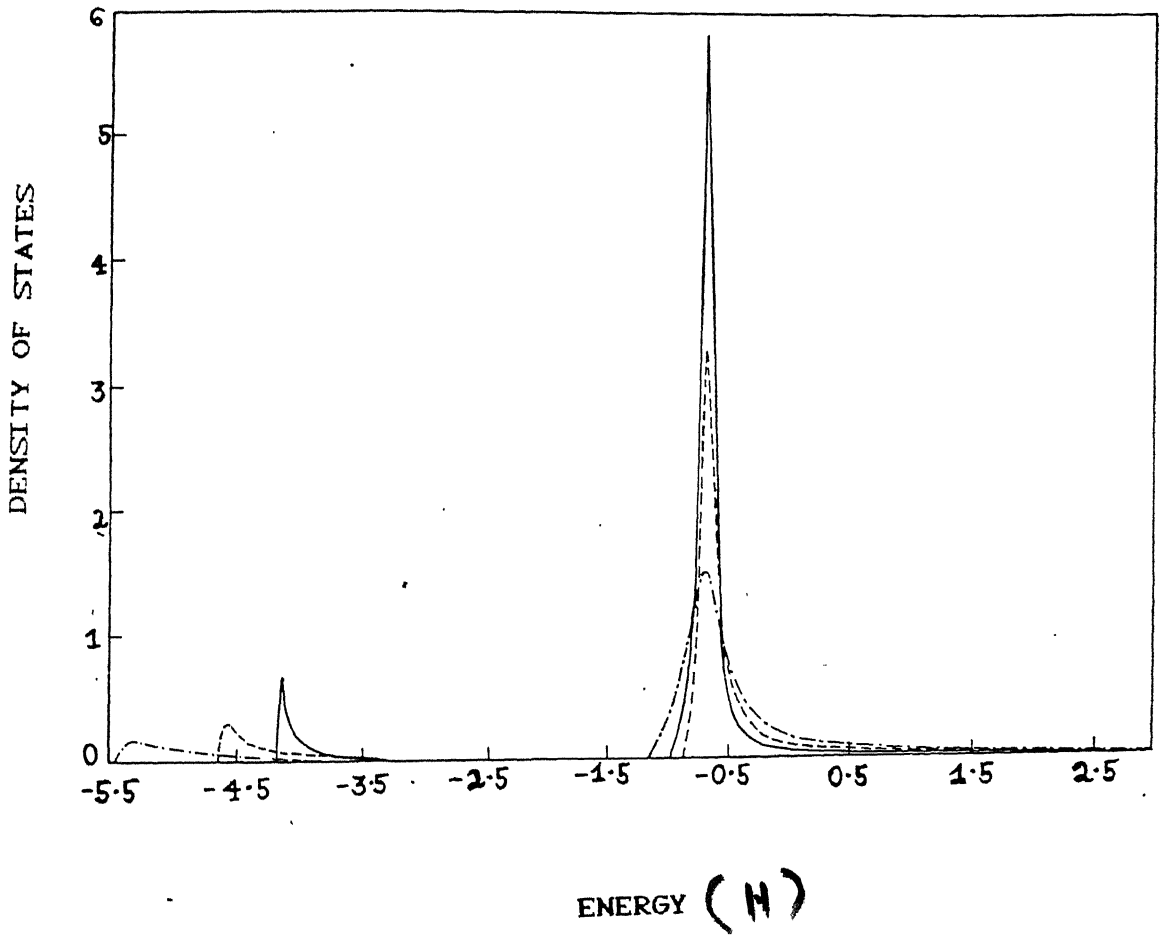

Figure 3.5 :(c) Densities of states for V_A=5.0 au, V_B = 1.0 au c=0.1 and with λ's as given in figure 3.1(a).

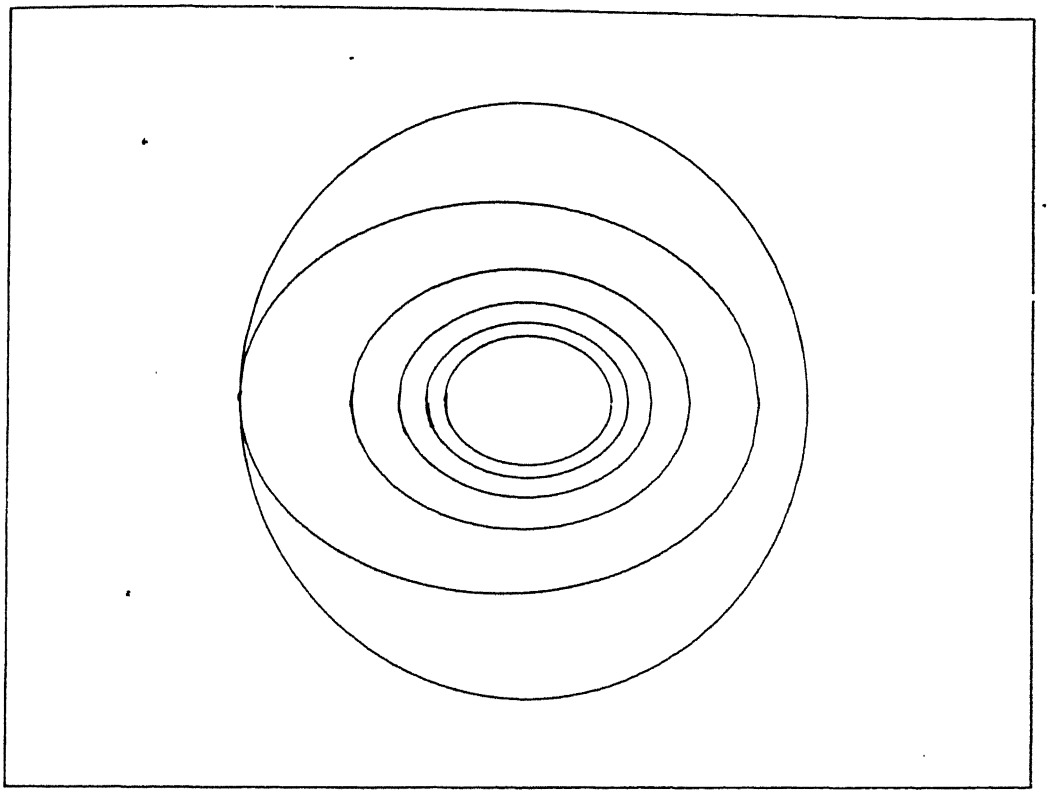

Figure 3.6 : Equipotential surfaces in subspace I.

CHAPTER IV

AN EMBEDDING-CPA FORMALISM IN ONE DIMENSION

The KKR method proposed four decades ago by Korringa (1947) and Kohn and Rostoker (1954) remains a powerful technique for accurate calculation of electronic band structure for pure metals. Later this method was adopted by Gyorffy and Stock to calculate the electronic band structure of random metallic alloys. Butler (1976) developed the one dimensional analog of KKR approach. In this chapter we review the one dimensional analog of KKR approach and then develop the Embedding-KKR-CPA formalism to calculate the electronic density of states for one dimensional random chain of flat potential wells.

4.1: KKR FORMALISM IN ONE DIMENSION

We consider a one dimensional system with Hamiltonian

$$H = -\frac{d^2}{dx^2} + U(x)$$

where

$$U(x) = \sum_n v_n(x-na) \qquad (4.1.1)$$

and the summation is over n atomic sites with lattice parameter a. We assume $v_n(x-na)$ to be symmetric and vanishing for $r=|x|$ greater than some muffin-tin radius r_{mt}. We also assume that the

distance between the centres of the potentials is great enough, so that they do not overlap. If the potential is situated at the origin then we have

$$v_n(x) = 0 \ , \ r = |x| > r_{mt} \ , \text{ where } \qquad r_{mt} < 1/2\ a$$

For a single symmetric potential satisfying equation (4.1.1) we have

$$\left[-\frac{d^2}{dx^2} + U(x) - E \right] \psi(x) = 0 \qquad (4.1.2)$$

We shall expand the wave function about the centre of the potential in terms of symmetric and antisymmetric functions, analogous to the spherical harmonics used in KKR theory:

$$Y_o(\hat{x}) = 1/\sqrt{2}$$
$$Y_1(\hat{x}) = (1/\sqrt{2}\ )\ \ \text{sign}(x) \qquad (4.1.3a)$$

We shall also need the one dimensional analogs of the spherical Bessel functions :

$$j_l(z) = \cos(z - l\pi/2\ ),\ l = 0,1$$
$$n_l(z) = \sin(z - l\pi/2\ ),\ l=0,1 \qquad (4.1.3b)$$

Now the wave function satisfying equation (4.1.2) can be written as

$$\psi(x) = 2 \sum_l a_l\ R_l(kr)\ Y_l(\hat{x}) \qquad (4.1.3c)$$

where $G_o(x,x')$ is the free electron Green function and

$$\tau^{mn}_{l_1 l_2} = t^m_{l_1}\delta_{l_1 l_2}\delta_{mn} + \sum_{l_3}\sum_{p\neq m} t^m_{l_1} G'_{l_1 l_3}(R_m - R_p)\tau^{pn}_{l_3 l_2} \qquad (4.1.5b)$$

is the scattering path operator introduced by Gyorffy and Stott.

Equation (4.1.5a) applies for any arrangement of non-overlapping muffin-tin potentials. If we restrict our consideration to identical scatterer on a lattice, then the scattering path operator may be written by means of a lattice Fourier transform,

$$\tau_{l_1 l_2}(k) = \frac{1}{N}\sum_m\sum_n \exp(-ik(m-n)a)\,\tau^{mn}_{l_1 l_2}$$

$$= t_{l_1}\delta_{l_1 l_2} + \sum_{l_3} t_{l_1} G'_{l_1 l_3}(k)\,\tau_{l_3 l_2}(k) \qquad (4.1.5c)$$

where

$$G'_{l_1 l_3}(k) = \sum_{p\neq o}\exp(-ikpa)\,G'_{l_1 l_3}(pa) \qquad (4.1.5d)$$

equation (4.1.5c) is a two by two matrix equation for τ which has the solution

$$(\tau^{-1})_{l_1 l_2} = t^{-1}_{l_1}\delta_{l_1 l_2} - G'_{l_1 l_2}(k) \qquad (4.1.5e)$$

The poles of scattering path operator are determined by the determinant equation : $\det(\tau^{-1}) = 0$, which are also the poles of

the Green function and thus the eigen values of the Hamiltonian.

Then

$$\det\,[t_l^{-1}\,\delta_{ll'} - G'_{l'}(k)] = 0 \qquad (4.1.6)$$

is the one dimensional analog of KKR equation. We are mainly interested in the Green function $G(x,x')$ when x and x' are both within the same Wigner-Seitz cell. Let us suppose that x and x' are both within the Wigner-Seitz cell at the origin (but in the zero potential muffin-tin plateau region). Then using the spherical harmonics expansion of all terms about the origin the Green function can be reduced to

$$G(x,x') = G_o(x,x') + \sum_l (ik)^{-2} h_l(kr) h_l(kr') t_l^o\, Y_l(\hat{x}) Y_l(\hat{x}')$$

$$+ \sum_{l_1 l_2} \left[j_{l_1}(kr) + (ik)^{-1} t_{l_1} h_{l_1}(kr) \right] Y_{l_1}(\hat{x}) G^{oo}_{l_1 l_2}$$

$$\left[j_{l_2}(kr') + (ik)^{-1} t_{l_2} h_{l_2}(kr') Y_{l_2}(\hat{x}') \right] \qquad (4.1.7a)$$

where we have used the relations

$$\tau^{oo}_{l_1 l_2} = t^o_{l_1}\,\delta_{l_1 l_2} + t^o_{l_1} G^{oo}_{l_1 l_2} t^o_{l_2}$$

$$\sum_{l_2} G'_{l_1 l_2}(k_m)\,\tau^{oo}_{l_2 l_3} = G^{oo}_{l_1 l_2} t^o_{l_2} \qquad (4.1.7b)$$

and

$$\sum_{l_2} \tau^{oo}_{l_1 l_2} G'_{l_2 l_3}(k_n) = t^o_{l_1} G^{oo}_{l_1 l_3}$$

and

$$G^{oo}_{l_1 l_2} = t^{-1}_{l_1}(\tau^{oo}_{l_1 l_2} - t_{l_1}\delta_{l_1 l_2})\, t^{-1}_{l_2} \qquad (4.1.7c)$$

For x and x′ both at one of the boundaries of the cell at the origin, expression (4.1.7a) reduces to

$$G(x,x') = \sum_l G_l(r,r')\, Y_l(\hat{x})Y_l(\hat{x}') \qquad (4.1.8a)$$

where

$$G_l(r,r') = \frac{R_l(kr_<)}{k \sin\delta_l}\left[j_l(kr_>) + \frac{R_l(kr_>)}{k \sin\delta_l}\,\tau^{oo}_{ll} \right] \qquad (4.1.8b)$$

We have to calculate $\tau^{oo}_{l_1 l_2}$, *i.e.*, the scattering path operator for a path which leaves from and returns to the origin. From equation (4.1.5c) and equation (4.1.5e) this is

$$\tau^{oo}_{l_1 l_2} = (a/2\pi)\int dk\, (t^{-1} - G'(k))^{-1}_{l_1 l_2} \qquad (4.1.9)$$

In one dimension taking only l = 0 and 1 partial waves in the expression the elements of this path operator matrix, $\tau^{oo}_{l_1 l_2}$ can be obtained as follows:

$$\tau^{oo}_{oo} = \frac{-k}{2\pi}\,\frac{\tan\delta_0}{1+\tan\delta_0\tan\delta_1}\int_{-\pi}^{+\pi}\frac{\cos\theta - f_1}{\cos\theta - x}\, d\theta$$

$$\tau^{oo}_{ii} = \frac{-k}{2\pi} \frac{\tan\delta_i}{1+\tan\delta_o\tan\delta_i} \int_{-\pi}^{+\pi} \frac{\cos\vartheta - f_o}{\cos\vartheta - x}\, d\vartheta$$

$$\tau^{oo}_{oi} = -\tau^{oo}_{io} = \frac{-k}{2\pi} \frac{\tan\delta_o\tan\delta_i}{1+\tan\delta_o\tan\delta_i} \int_{-\pi}^{+\pi} \frac{i\,\sin\vartheta}{\cos\vartheta - x}\, d\vartheta$$

where

$$x = \frac{\cos(\varphi+\delta_o+\delta_i)}{\cos(\delta_o-\delta_i)}$$

$$f_o = \cos\varphi - \tan\delta_o \sin\varphi$$

$$f_i = \cos\varphi - \tan\delta_i \sin\varphi$$

$$\varphi = ka$$

(4.1.10)

The off-diagonal elements $\tau^{oo}_{oi} = \tau^{oo}_{io} = 0$, because of the odd parity of the integrand. So the scattering path operator matrix in one dimension is

$$\tau^{oo}_{l_1 l_2} = \begin{bmatrix} \tau^{oo}_{oo} & 0 \\ 0 & \tau^{oo}_{ii} \end{bmatrix}$$

Making change in the variable $z = \exp(i\vartheta)$, the integrals (4.1.10) and can be performed integrating around an unit circle in the following way:

$$I = \frac{1}{2\pi} \int_{-\pi}^{+\pi} \frac{\cos\vartheta - f}{\cos\vartheta - x}\, d\vartheta = \frac{1}{2\pi i} \oint \frac{dz}{z} \frac{z^2 - 2fz + 1}{z^2 - 2xz + 1}$$

(4.1.11)

The integrand of this has three simple poles, $z=0$, $z=z_<$ and $z=z_>$ where $z_<z_>=1$. For x real and less than 1 both $z_<$ and $z_>$ will be on the unit circle. However if we let E have a positive imaginary part, one of the pair between $z_<$ and $z_>$ will move outside and the other one inside the unit circle to satisfy the relation $z_<z_>= 1$. Thus equation (4.1.11) becomes

$$I = 1 \pm \frac{(x-f)}{(x^2-1)^{1/2}}$$

The sign is uniquely determined by giving E a small positive imaginary part and seeing which of the two roots $z_<$ or $z_>$ lies inside the unit circle in complex energy plane. The path operators will become

$$\tau_{oo}^{oo} = -k \frac{\tan\delta_o}{1+\tan\delta_o\tan\delta_1} I(x,f_1)$$

$$\tau_{ii}^{oo} = -k \frac{\tan\delta_1}{1+\tan\delta_o\tan\delta_1} I(x,f_o)$$

(4.1.12)

4.2: KKR-CPA FORMALISM IN ONE DIMENSION

Thus the one dimensional analog of KKR formalism developed by Butler gives the Green function for a single scatterer. When we apply Embedding method to one dimensional arrays of flat potentials subspace I will be a periodic system of identical

scatterers. It was suggested by Anderson and McMillan (1967), for liquid metals, that the Green function within the Wigner-Seitz cell at the origin for a periodic system is equal to that for a single scatterer in a uniform medium.

According to the Embedding theory, subspace I in one dimensional arrays of flat potentials model can be treated as a single impurity problem in an effective medium and the Green function with Neumann boundary condition at the interface S of the two subspaces I and II can be easily obtained.

The CPA can be derived requiring that the Green function for a system having scattering amplitudes t_A and t_B at the origin and the coherent scattering amplitude t_C at all other sites be equal on the average to the Green function for a system having t_C on all sites. Equivalently this can be written as

$$c_A \tau^{oo}_{C,A} + c_B \tau^{oo}_{C,B} = \tau^{oo}_C \qquad (4.2.1)$$

where τ^{oo}_C is given by equation (4.1.12) with $\tan\delta_l = \tan\delta^C_l$ and

$$\tau^{oo}_{c,A,ll} = (\tau^{oo\,-1}_{c,ll} + t^{-1}_{A,l} - t^{-1}_{c,l})^{-1}$$

Substituting one into the other yields an equation for on-energy shell t matrix, t_C:

$$t^{-1}_{c,l} = c_A t^{-1}_{A,l} + c_B t^{-1}_{B,l} + (t^{-1}_{c,l} - t^{-1}_{A,l})\, \tau^{oo}_{c,ll} (t^{-1}_{c,l} - t^{-1}_{A,l}) \qquad (4.2.2)$$

The inverse of the on-energy shell t matrix for a one dimensional array of flat potentials can be calculated to be of the form

$$t^{-1}_{c,l} = -k\,[\cot\delta_l - i]. \qquad (4.2.3)$$

Equation (4.2.2) is an alternative form of the CPA equation for random binary alloys. To solve this self-consistently a suitable initial choice of $t^{-1}_{c,l} = c_A\, t^{-1}_{A,l} + c_B\, t^{-1}_{B,l}$ is made and using in equation (4.2.3) we can calculate the phase shifts and substituting in equation (4.1.12) an initial value of $\tau^{oo}_{c,ll}$ can be calculated. Substituting these values in equation (4.2.2) we obtain a new value of $t^{-1}_{c,l}$. This goes iteratively until τ^{oo}_{ll} converges. Now we can calculate our Green function of subspace I at the interface, substituting the above τ^{oo}_{ll}. $R_l(kr)$ and $j_l(kr)$ are defined in equation (4.1.3d) and (4.1.3b) whereas the phase dependent terms are obtained from $t^{-1}_{c,l}$.

4.3 : EMBEDDING - KKR- CPA FORMALISM IN ONE DIMENSION

Here we are going to develop an Embedding-KKR-CPA theory in one dimension. The one dimensional space will be divided into two subspaces, *i.e.*, I and II with an interface S at $|x| = r_s$ as shown in figure(4.1).

Where $\Psi(x)$ is the eigen function of the Hamiltonian H of the whole one dimensional space satisfying the Schrödinger equation,

$$H\,\Psi(x) = E\,\Psi(x) \tag{4.3.1}$$

with energy eigenvalue E.

To solve the Schrödinger Equation in the region I we find the expectation value of the energy of the wave function $\Psi(x)$ of the full space, defined in subspace I as a trial wave function $\phi(x)$ and in the subspace II as the exact solution $\psi(x)$ of the Schrödinger equation at same energy E with an extra condition that the solution matches correctly on the boundary surface S :

$$\left[-\frac{d^2}{dx^2} + U(x) - E\right]\psi(x) = 0 \tag{4.3.2a}$$

and

$$\psi(x_s) = \phi(x_s) \tag{4.3.2b}$$

The energy expectation value of the Hamiltonian of the full space is

$$E = \frac{\int_{-\infty}^{\infty} dx\ \Psi^*(x) H \Psi(x)}{\int_{-\infty}^{\infty} dx\ \Psi^*(x)\Psi(x)} \tag{4.3.3}$$

Because of the discontinuity of the derivative of the wave function at the interface S we take an ε neighbourhood of the interface S to evaluate the integrals in subspace I of equation (4.3.3) and then take the limit ε to be zero as shown in the figure (4.2).

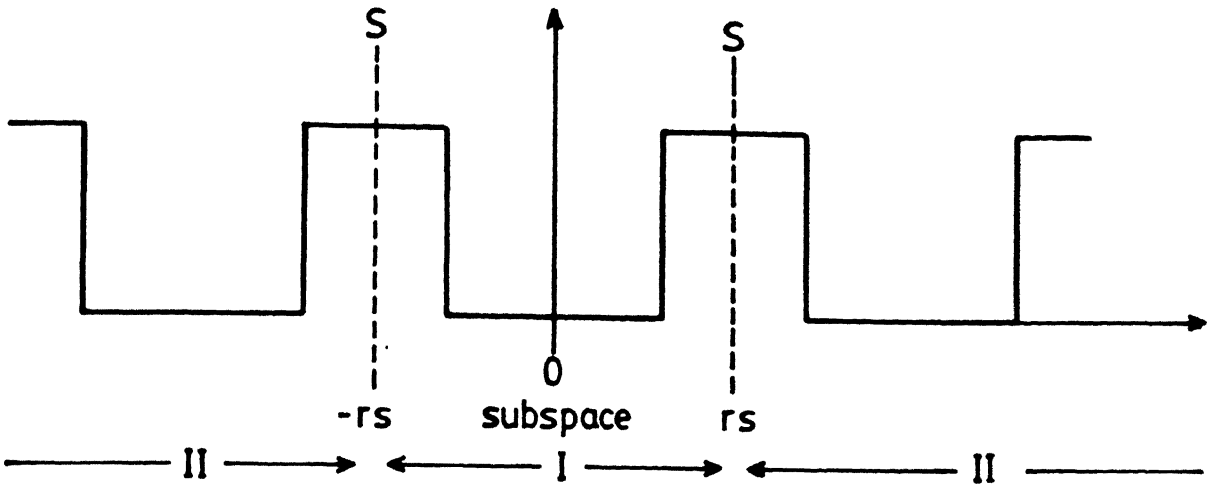

Figure 4.1 : Partition of one dimensional space into two subspaces, i.e, I & II.

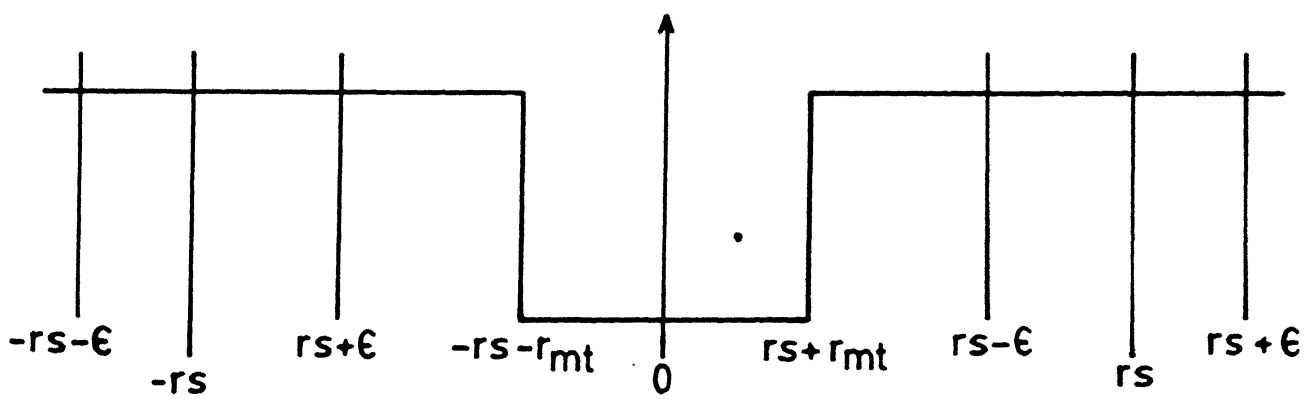

Figure 4.2 : Epsilon neighbourhood of subspace I.

Thus substituting equation (4.3.2a) in equation (4.3.3) we obtain :

$$E\int_{-\infty}^{-r_s-\varepsilon} dx\ \Psi^*(x)\Psi(x) + E\int_{-r_s-\varepsilon}^{r_s+\varepsilon} dx\ \Psi^*(x)\Psi(x) + E\int_{r_s+\varepsilon}^{\infty} dx\ \Psi^*(x)\Psi(x)$$

$$= E\int_{-\infty}^{-r_s-\varepsilon} dx\ \Psi^*(x)\Psi(x) + \int_{-r_s-\varepsilon}^{-r_s+\varepsilon} dx\ \Psi^*(x)H\Psi(x) + \int_{-r_s+\varepsilon}^{r_s-\varepsilon} dx\ \phi^*(x)H\phi(x)$$

$$+ \int_{r_s-\varepsilon}^{r_s+\varepsilon} dx\ \Psi^*(x)H\Psi(x) + E\int_{r_s+\varepsilon}^{\infty} dx\ \Psi^*(x)\Psi(x)$$

which can be reduced to

$$E\int_{-r_s-\varepsilon}^{r_s+\varepsilon} dx\ \Psi^*(x)\Psi(x) = \int_{-r_s-\varepsilon}^{-r_s+\varepsilon} dx\ \Psi^*(x)H\Psi(x) + \int_{-r_s+\varepsilon}^{r_s-\varepsilon} dx\ \phi^*(x)H\phi(x)$$

$$+ \int_{r_s-\varepsilon}^{r_s+\varepsilon} dx\ \Psi^*(x)H\Psi(x)$$

(4.3.4)

Let us now evaluate each integral separately. The first term will be

$$\int_{-r_s-\varepsilon}^{-r_s+\varepsilon} dx\ \Psi^*(x)H\Psi(x) = \int_{-r_s-\varepsilon}^{-r_s+\varepsilon} dx\ \Psi^*(x)\left[-\frac{d^2}{dx^2}\right]\Psi(x)$$

$$= -\Psi^*(x)\,\frac{d}{dx}\Psi(x)\Big|_{-r_s-\varepsilon}^{-r_s+\varepsilon} + \int_{-r_s-\varepsilon}^{-r_s+\varepsilon} dx\,\frac{d}{dx}\Psi^*(x)\,\frac{d}{dx}\Psi(x)$$

With limit ε going to 0, equation 4.3.3 becomes

$$= -\left[\phi^*(-r_s)\frac{d}{dx}\phi(x)\Big|_{-r_s} - \psi^*(-r_s)\frac{d}{dx}\psi(x)\Big|_{-r_s}\right]$$

Similarly the third term will be

$$\int_{r_s-\varepsilon}^{r_s+\varepsilon} dx\;\Psi^*(x)\left[-\frac{d^2}{dx^2}\right]\Psi(x) = -\Psi^*(x)\frac{d}{dx}\Psi(x)\Big|_{r_s-\varepsilon}^{r_s+\varepsilon}$$

$$+\int_{r_s-\varepsilon}^{r_s+\varepsilon} dx\,\frac{d}{dx}\Psi^*(x)\frac{d}{dx}\Psi(x)$$

$$= -\left[\psi^*(r_s)\frac{d}{dx}\psi(x)\Big|_{r_s} - \phi^*(r_s)\frac{d}{dx}\phi(x)\Big|_{r_s}\right]$$

Now in the limit ε going to 0, substituting these two in equation (4.3.4) we obtain

$$E\int_{-r_s}^{r_s} dx\;\phi^*(x)\phi(x) = \int_{-r_s}^{r_s} dx\;\phi^*(x)H\phi(x)$$

$$-\left[\phi^*(-r_s)\frac{d}{dx}\phi(x)\Big|_{-r_s} - \psi^*(-r_s)\frac{d}{dx}\psi(x)\Big|_{-r_s}\right]$$

$$-\left[\psi^*(r_s)\frac{d}{dx}\psi(x)\Big|_{r_s} - \phi^*(r_s)\frac{d}{dx}\phi(x)\Big|_{r_s}\right]$$

(4.3.5)

According to Embedding theory now we express the derivative $\frac{d}{dx}\psi(x)\Big|_{x=\pm r_s}$ in subspace II in terms of the trial wave function $\phi(r_s)$ in subspace I by using the Green function $G^{II}(x,x')$ for region II, satisfying the equation

$$\left[-\frac{d^2}{dx^2} + U(x)-E\right]G^{II}(x,x') = \delta(x-x') \tag{4.3.6}$$

where x and x' are in region II, *i.e.*, $|x| > r_s$. Multiplying equation (4.3.2a) by $G^{II}(x,x')$ and equation (4.3.6) by $\psi(x)$ and substituting one from the other we get

$$\left[-\frac{d^2}{dx^2}\,\psi(x)\right]G^{II}(x,x') + \left[\frac{d^2}{dx^2}\,G^{II}(x,x')\right]\psi(x) = -\delta(x-x')\psi(x) \tag{4.3.7}$$

Integrating through the region $|x| > r_s$, exchanging x and x', then substituting the boundary condition on the surface the above equation will reduces to

$$\psi(x) = G^{II}(x',x)\frac{d}{dx'}\psi(x')\Big|_{-\infty}^{-r_s-\varepsilon} + G^{II}(x',x)\frac{d}{dx'}\psi(x')\Big|_{r_s+\varepsilon}^{\infty}$$

With limit ε going to zero this equation becomes

$$\psi(x) = G^{II}(-r_s,x)\frac{d}{dn_s}\psi(x')\Big|_{-r_s} - G^{II}(r_s,x)\frac{d}{dn_s}\psi(x')\Big|_{r_s}$$

So the wave function at interface of the two subspaces will be

$$\psi(r_s) = \phi(r_s) = G^{II}(-r_s,r_s)\frac{d}{dn_s'}\psi(x')\Big|_{-r_s} - G^{II}(r_s,r_s)\frac{d}{dn_s'}\psi(x')\Big|_{r_s}$$

(4.3.8a)

$$\psi(-r_s) = \phi(-r_s) = G^{II}(-r_s,-r_s)\frac{d}{dn_s'}\psi(x')\Big|_{-r_s} - G^{II}(r_s,-r_s)\frac{d}{dn_s'}\psi(x')\Big|_{r_s}$$

(4.3.8b)

Multiplying equation (4.3.8a) by $G^{II}(-r_s,-r_s)$ and equation (4.3.8b) by $G^{II}(-r_s,r_s)$ and subtracting one from the other we obtain

$$\phi(r_s)G^{II}(-r_s,-r_s)-\phi(-r_s)G^{II}(-r_s,r_s)$$

$$= \left[G^{II}(r_s,-r_s)G^{II}(-r_s,r_s)-G^{II}(r_s,r_s)G^{II}(-r_s,-r_s)\right]\frac{d}{dx'}\psi(x')\Big|_{r_s}$$

(4.3.9)

Again substituting D for the bracketed term on the right hand side of equation (4.3.9) we get

$$\frac{d}{dn_s'}\psi(x')\Big|_{r_s} = \frac{1}{D}\left[\phi(r_s)G^{II}(-r_s,-r_s)-\phi(-r_s)G^{II}(-r_s,r_s)\right]$$

(4.3.10a)

Similarly multiplying equation (4.3.8a) by $G^{II}(r_s,-r_s)$ and equation (4.3.8b) by $G^{II}(r_s,r_s)$ and substituting one into the other we get

$$\frac{d}{dn'}\psi(x')\Big|_{-r_s} = \frac{1}{D}\left[\phi(r_s)G^{II}(r_s,-r_s)-\phi(-r_s)G^{II}(r_s,r_s)\right]$$

(4.3.10b)

substituting these two expressions in equation(4.3.5) we get

$$E\int_{-r_s}^{r_s} dx\ \phi^*(x)\phi(x) = \int_{-r_s}^{r_s} dx\ \phi^*(x)H\phi(x)$$

$$- \left[\ \phi^*(-r_s)\frac{\partial}{\partial n_s}\phi(x)\Big|_{-r_s} - \phi^*(r_s)\frac{\partial}{\partial n_s}\phi(x)\Big|_{r_s}\right]$$

$$-\left[\phi^{*}(r_s)\frac{1}{D}\left[G^{II}(-r_s,-r_s)\phi(r_s)-G^{II}(-r_s,r_s)\phi(-r_s)\right]\right.$$

$$\left.-\phi^{*}(-r_s)\frac{1}{D}\left[G^{II}(r_s,-r_s)\phi(r_s)-G^{II}(r_s,r_s)\phi(-r_s)\right]\right] \qquad (4.3.11)$$

This expression gives us E purely in terms of a trial function $\phi(x)$ defined in subspace I and on the interface S. The variational minimization of E with respect to the trial wave function $\phi^{*}(x)$ i.e.,

$$\frac{\delta E}{\delta \phi^{*}(x)} = 0$$

gives

$$E\ \phi(x) = \left[-\frac{d^2}{dx^2} + V_I(x)\right]\phi(x)$$

$$-\left[\delta(n+n_s)\frac{d}{dn_s}\phi(x) - \delta(n-n_s)\frac{d}{dn_s}\phi(x)\right]$$

$$-\left[\delta(n-n_s)\frac{1}{D}\left[G^{II}(-r_s,-r_s)\phi(r_s)-G^{II}(-r_s,r_s)\phi(-r_s)\right]\right.$$

$$\left.-\delta(n+n_s)\frac{1}{D}\left[G^{II}(r_s,-r_s)\phi(r_s)-G^{II}(r_s,r_s)\phi(-r_s)\right]\right] \qquad (4.3.12)$$

This is the one dimensional analog of Embedded Schrödinger equation that acts on the subspace I alone and the effect of larger subspace II appears as the surface potential operator

$$\left[\delta(n-n_s)\frac{1}{D}\,G(-r_s,-r_s)-\delta(n+n_s)\frac{1}{D}\,G(r_s,-r_s)\right]+\left[\delta(n-n_s)\frac{1}{D}\right.$$

$$\left.G(-r_s,r_s)+\delta(n+n_s)\frac{1}{D}\,G(r_s,r_s)\right]$$

The terms $\delta(n+n_s)(\partial/\partial n_s)$ and $\delta(n-n_s)(\partial/\partial n_s)$ ensure that the effective Hamiltonian remains Hermitian in region I alone.

4.3.1: RESOLVENT OPERATOR IN ONE DIMENSION

For actual calculation of one dimensional resolvent operator we need a representation of effective Hamiltonian in a suitable basis. So we expand our trial wave function in subspace I in terms of a countable basis $\chi(x)$ which spans the subspace I and reflects the symmetry of the solution we wish to study in I.

$$\phi(x)=\sum_l a_l \chi_l \tag{4.3.13}$$

Using this basis in equation (4.3.12) and minimising E with respect to variation in a_l, the effective Schrödinger equation in one-dimension can be written as

$$\sum_k H_{lk}\, a_k = E \sum_k O_{lk}\, a_k \tag{4.3.14}$$

where

$$H_{lk} = \int_{-r_s}^{r_s} dx\ \chi_l^*(x)\left[-\frac{d^2}{dx^2}+V_I(x)\right]\chi_k(x)$$

$$-\left[\chi_l^*(-r_s)\left(\frac{d}{dx}\chi_k(x)\Big|_{-r_s}\right)-\chi_l^*(r_s)\left(\frac{d}{dx}\chi_k(x)\Big|_{r_s}\right)\right]$$

$$-\left[\chi_l^*(r_s)\left\{\frac{1}{D}\left[G^{II}(-r_s,-r_s)\chi(r_s)-G^{II}(-r_s,r_s)\chi(-r_s)\right]\right\}\right.$$

$$\left.-\chi^*(-r_s)\left\{\frac{1}{D}\left[G^{II}(r_s,-r_s)\chi(r_s)-G^{II}(r_s,r_s)\chi(-r_s)\right]\right\}\right] \tag{4.3.14}$$

and the overlap matrix is

$$O_{lk} = \int_{-r_s}^{r_s} dx\ \chi_l^*(x)\ \chi_k(x)$$

(4.3.15)

Here the Green function in subspace II can be expanded as

$$G^{II}(x,x') = \sum_l G_l(r,r') Y_l(\hat{x}) Y_l(\hat{x}')$$

(4.3.16a)

where

$$G_l(r,r') = \frac{1}{k \sin\delta_l}\left[R_l(kr_<) - \frac{R_l'(kr_s)}{F_l'(kr_s)} F_l(kr_>)\right]$$

(4.3.16b)

and

$$F_l(kr) = \left[j_l(kr) + \frac{R_l(kr)}{k \sin\delta_l} \tau_{ll}^{oo}\right]$$

(4.3.16c)

Now analogous to the three dimensional embedded theory the matrix representation of the embedded Green function or resolvent operator in one dimension will be

$$G_{lk} = (H-EO)^{-1}_{lk}$$

(4.3.17)

where the local density of state is defined in chapter II.

CHAPTER V

ONE DIMENSIONAL MODELS

In this chapter we shall illustrate our one dimensional analog of Embedding formalism taking single and double muffin-tin potential wells of the binary alloy type with probabilities c and (1-c) and potentials $V_I(r) = -V_A$ or $-V_B$ in the region I. In region II we replace translationally symmetric muffin-tin potential of the binary alloy type by an effective CPA medium and evaluate the path operator and surface Green function using KKR-CPA theory, Butler (1976). Let us now calculate the local electron density of states embedding single and pair muffin-tin potential in the one dimensional effective CPA medium.

5.1 : SINGLE MUFFIN-TIN POTENTIAL IN SUBSPACE I

We choose our single member basis function to be of the form $\chi(x) = 2(1/N)\ (a_0\chi(x)+a_1\chi(x))$ in subspace I, where N is the normalization factor; a_0 and a_1 are given by $e^{i\delta_0}$ and $e^{i\delta_1}$ respectively for l = 0 and 1 partial wave states. Expanding $\chi_0(x)$ and $\chi_1(x)$ explicitly in terms of equations (4.1.3a), (4.1.3b), (4.1.3d) we obtain

$$\chi_0(x) = R_0(r)\ Y_0(\hat{x})$$

with

$$R_0(r) = \cos(kr+\delta_0) \qquad r_0 < r < r_s$$
$$= \cos \varkappa r \qquad -r_0 < r < r_0$$

$$= \cos(kr-\delta_0) \qquad -r_s < r < -r_0$$

(5.1.1)

and $\chi_l(x) = R_l(r)\, Y_l(\hat{x})$

with

$$\begin{aligned} R_l(r) &= \sin(kr+\delta_l) && r_0 < r < r_s \\ &= \sin \varkappa r && 0 < r < r_0 \\ &= -\sin \varkappa r && -r_0 < r < 0 \\ &= \sin(kr-\delta_l) && -r_s < r < -r_0 \end{aligned}$$

(5.1.2)

with $\varkappa^2 = (E-V_I(r))$, where $V_I(r)$ can either $-V_A$ or $-V_B$ and $k^2 = E$. The phase shifts for l=0 and l=1 partial wave states can be calculated respectively from the relations given by equation (5.1.3) :

$$\tan\delta_0 = (\varkappa \tan \varkappa r_0 - k \tan k r_0)(k + \varkappa \tan k r_0 \tan \varkappa r_0)^{-1}$$

$$\tan\delta_1 = (k \tan \varkappa r_0 - \varkappa \tan \varkappa r_0)(k \tan \varkappa r_0 \tan \varkappa r_0 + \varkappa)^{-1}$$

(5.1.3)

The normalisation factor can be obtained from

$$N^2 = 4 \int_{-r_s}^{r_s} dx\, \chi^*(x)\, \chi(x)$$

(5.1.4)

In this basis the overlap element is

$$0 = \frac{4}{N^2} \int_{-r_s}^{r_s} dx\, \chi^*(x)\, \chi(x) ,$$

(5.1.5)

where we have calculated these integrals numerically using

computer. The Hamiltonian is

$$H = E\,O + (4k/N^2)\left[-\cos(kr_s+\delta_0)\sin(kr_s+\delta_0) + \cos(kr_s+\delta_1)\sin(kr_s+\delta_1)\right] + (4/N^2)\left[\frac{\cos^2(kr_s+\delta_0)}{G_0(r_s,r_s)} + \frac{\sin^2(kr_s+\delta_1)}{G_1(r_s,r_s)}\right] \quad (5.1.6)$$

where the Green function of the effective CPA medium on the interface S is given by equations (4.3.16b) and (4.3.16c) and the path operator by the equation (4.1.12) . Giving a small positive imaginary part ($10^{-\delta}$) to the energy we get analytic density of states at all energies except at zero and a few other values of energies, because our path operator calculation fails to work at these points.

The local density of states is

$$n(r,E) = -\frac{c}{\pi}\,\mathrm{Im}\,\frac{O_A}{EO_A - H_A} - \frac{(1-c)}{\pi}\,\mathrm{Im}\,\frac{O_B}{EO_B - H_B} \quad (5.1.7)$$

5.1.1: RESULTS

In order to identify the structures in the negative energy range of the density of states of (10% -90%) composition of the binary alloy, we compare the local density of states of the alloy as in figure 5.1(a) with the local density of states in A and B

atoms in the alloy as shown in figure 5.1(b) and 5.1(c) respectively. We have taken V_A = -0.3 au, V_B = -0.5 au. We identify A_1, A_2 as peaks associated with the A constituents as in figure 5.1(b) and B_1,B_2 with the B constituents as in figure 5.1(c).

There is some overlap between the two, leading to widening of the structures, to form a three peaked band. Peaks A_1 and B_1 are wide peaks whereas A_2 is a sharp one. The peak A_2 sits on a narrow band, coming from the medium. This is separated from the previous structure by a narrow gap. The positive energy bands have long widths, so that their smoother structures are not identifiable. The characteristic Van Hove singularity structures (widened by disorder) are well describable.

We analyse the (50% - 50%) composition of the negative energy density of states of 1CPA, shown in figure 5.2(a) comparing with the density of states of A and B constituents shown in figure 5.2(b) and 5.2(c) respectively. We find there are three structures. The left most A_1 and right most A_2 structures are from A constituents of the alloy whereas the single peak of B constituent is B_1 situated in between and is sharper than A_1 and A_2. All the negative energy structures are well separated. If we analyse the peaks of B constituent we find there is a sharp delta function like peak and a small sharp peak. In between these two peaks the density of states does not converge because our path operator calculation fail to work at these energy points.

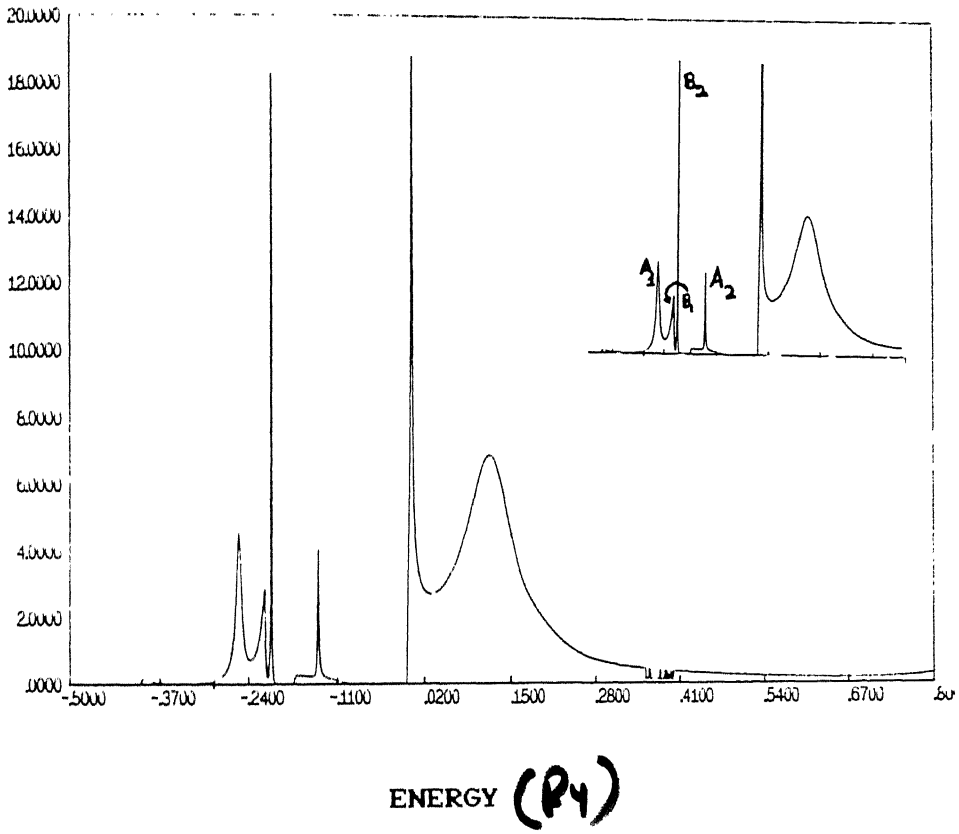

Figure 5.1a : ICPA, densities of states for V_A = -0.3 au, V_B = -0.5 au, and c = 0.1.

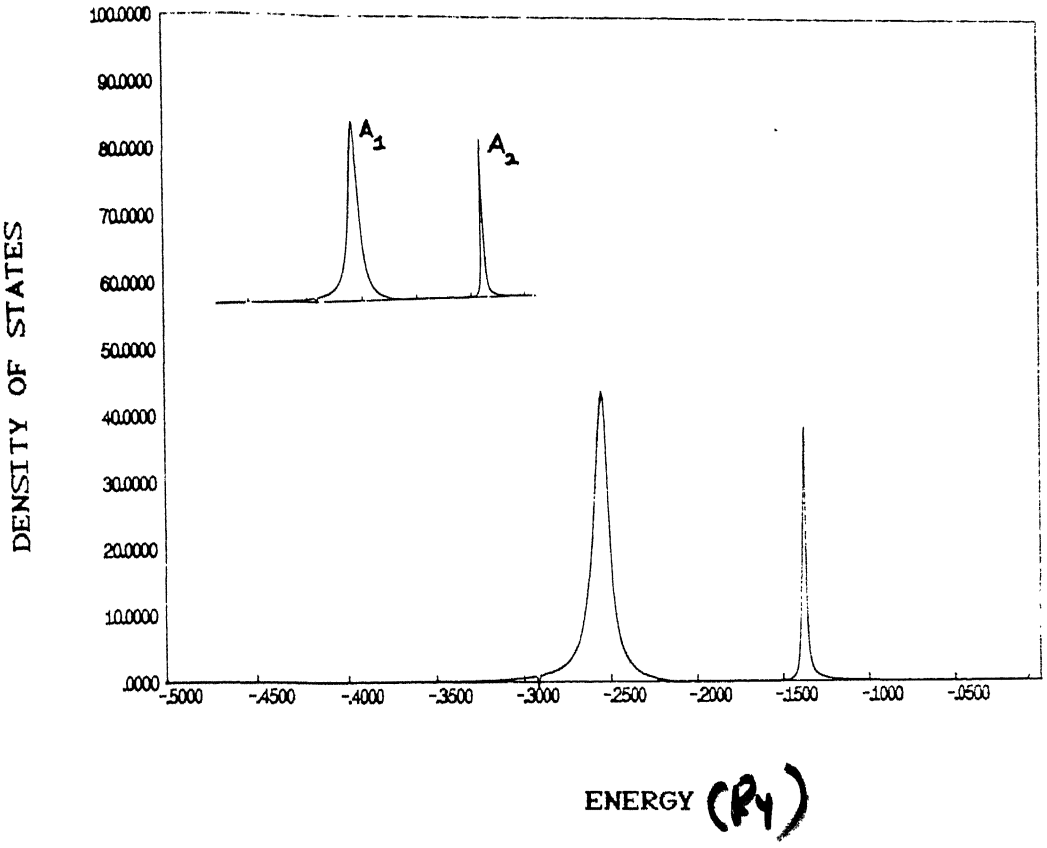

Figure 5.1b : ICPA, negative energy partial densities of states of the A constituent of the binary alloy for V_A=-0.3 au.

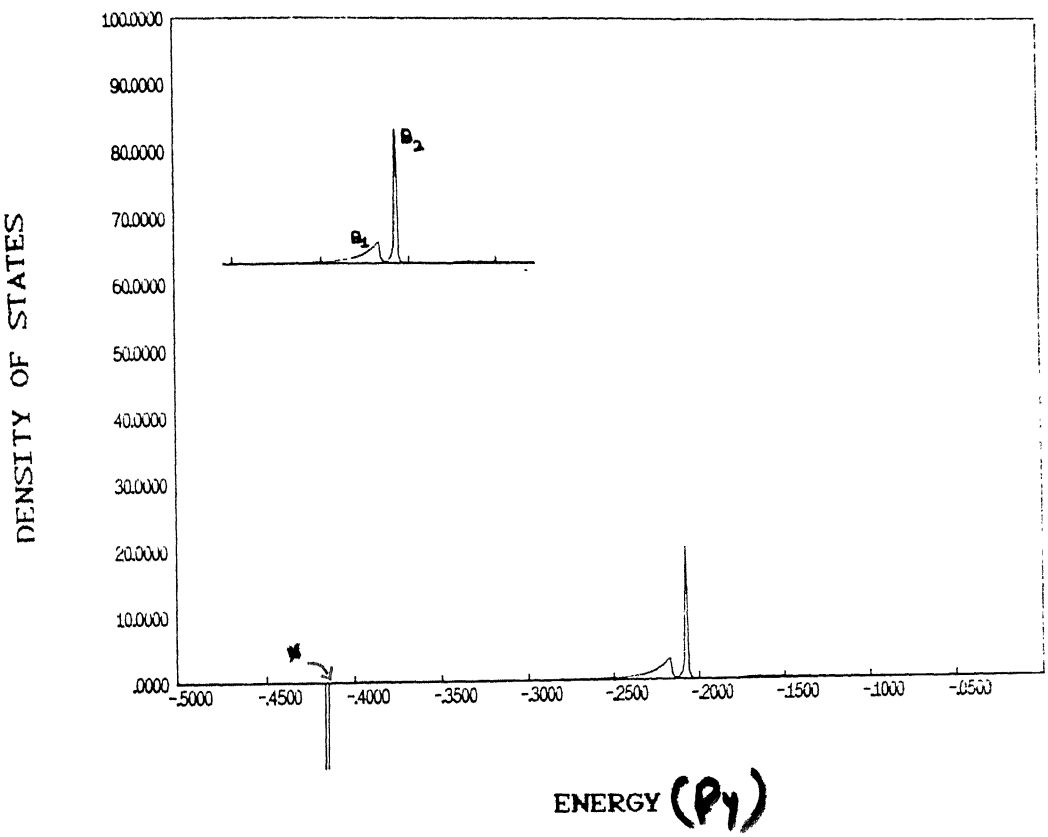

Figure 5.1c : ICPA, negative energy partial densities of states of the B constituent of the binary alloy for V_B=-0.5 au.

* Retenu à page 88

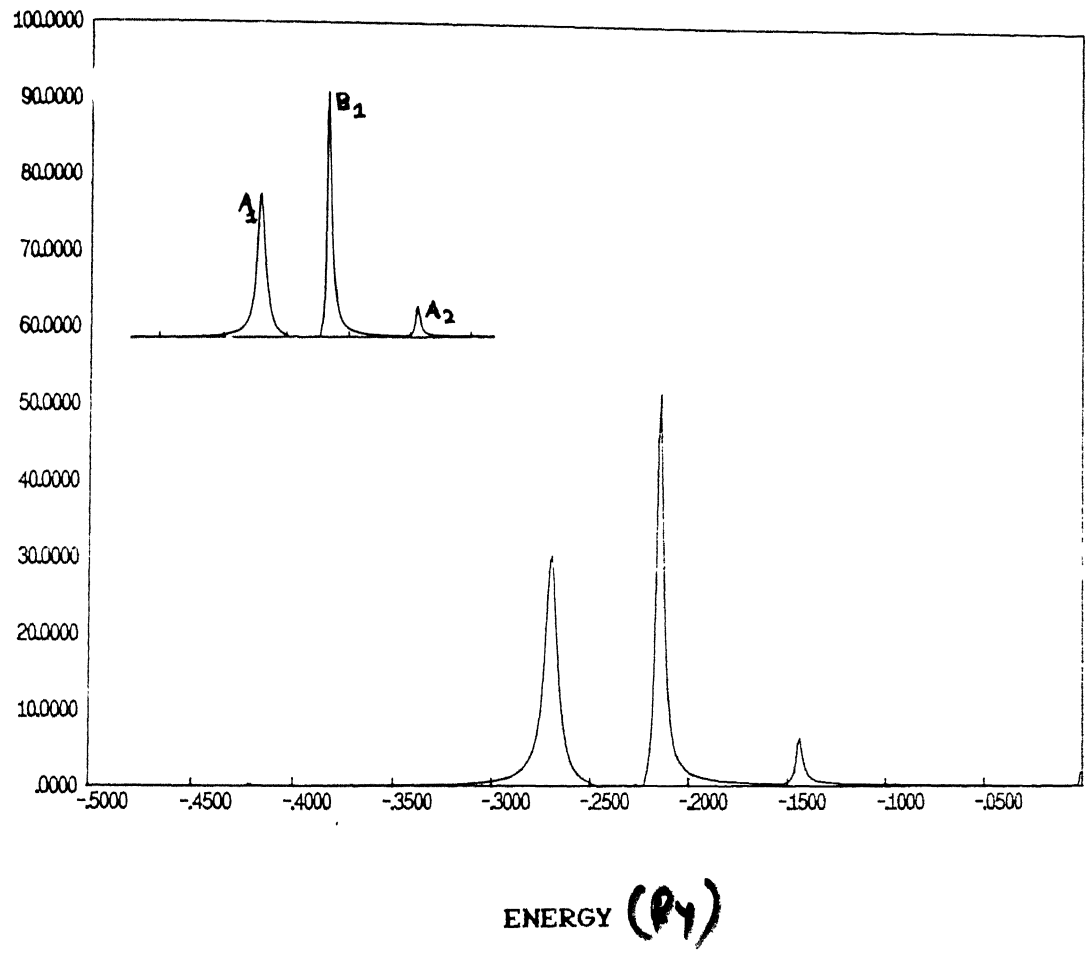

Figure 5.2a : 1CPA, negative energy densities of states for V_A=-0.3 au, V_B=-0.5 au and c=0.5.

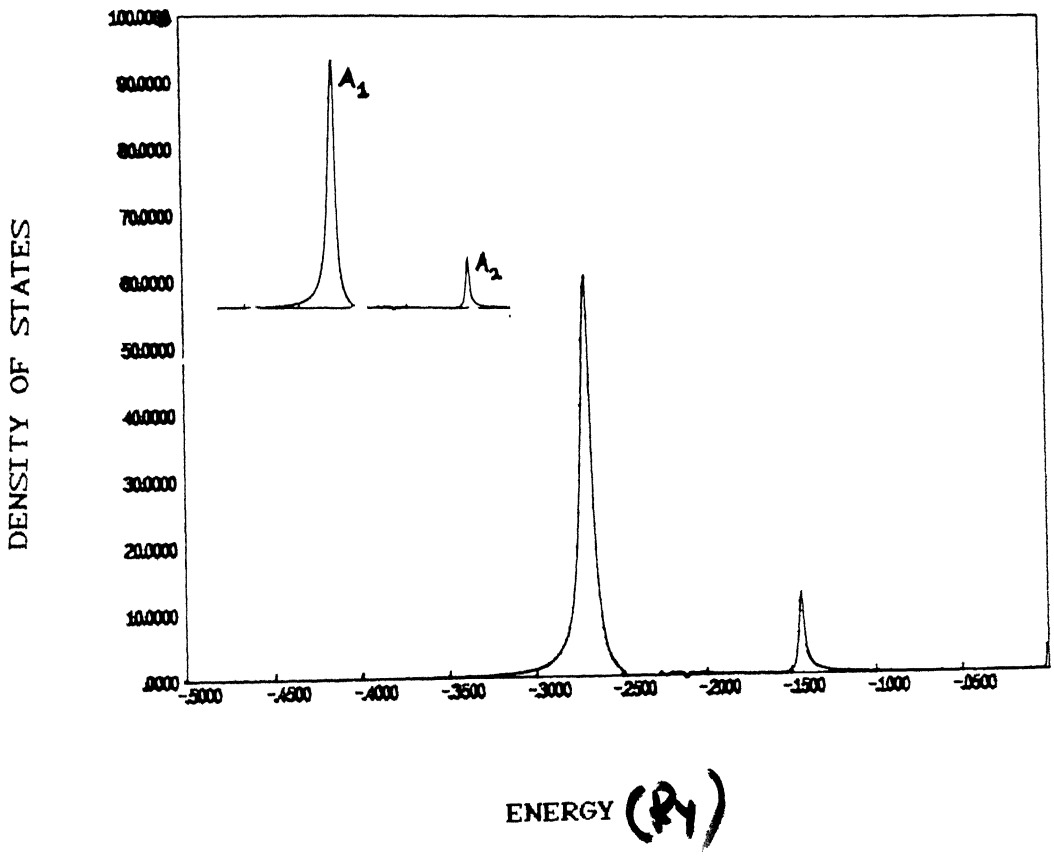

Figure 5.2b: ICPA, negative energy partial densities of states of the A constituent of binary alloy for V_A=-0.3 au.

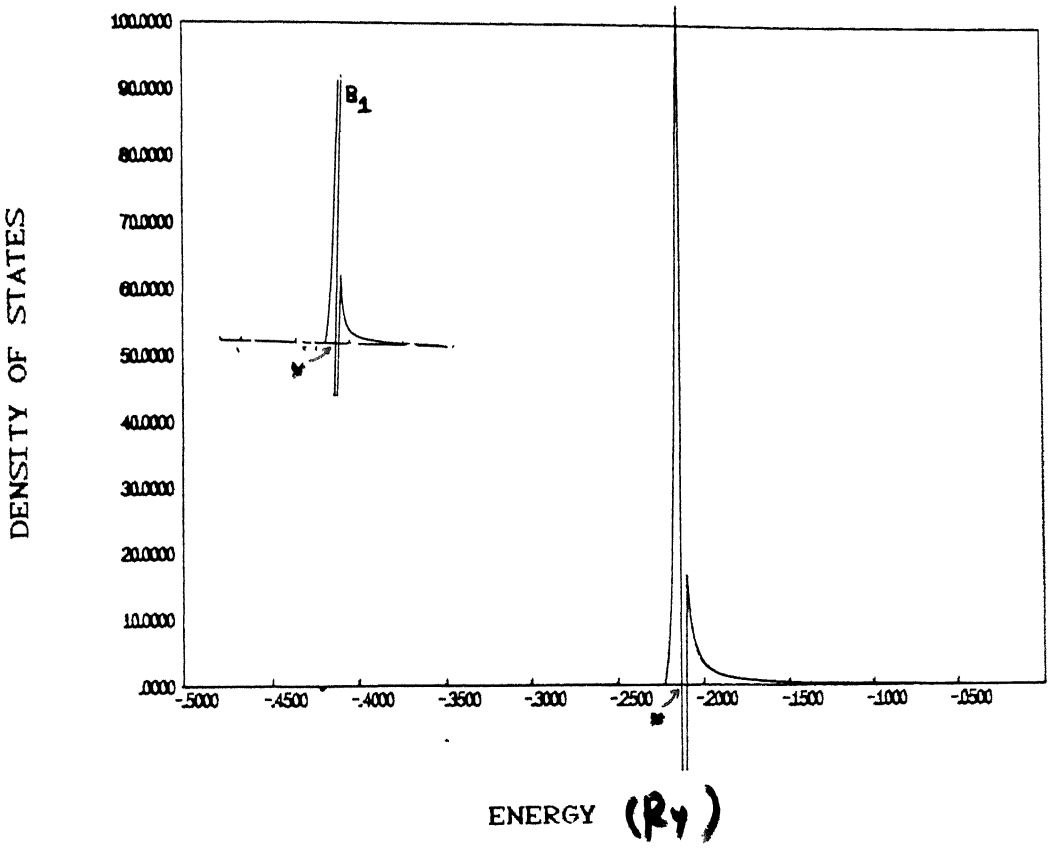

Figure 5.2c :1CPA, negative energy partial densities of states of the B constituent of binary alloy for V_B=-0.5 au.

* Returned to page 88.

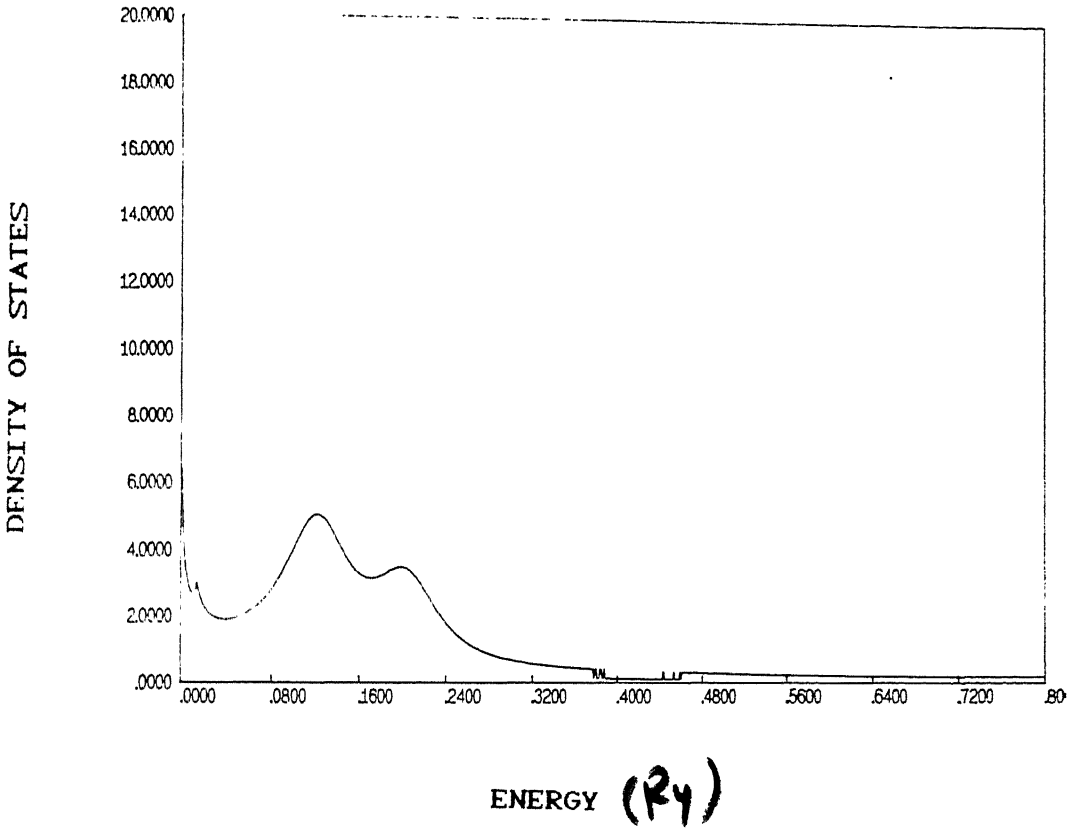

Figure 5.2d: ICPA, positive energy densities of states for V_A=-0.3 au, V_B=-0.5 au and c=0.5.

It is pertinent to mention here that the method for choosing the roots $z_>$, $z_<$ in the calculation of the path operator occasionally fails in the negative energy region. Whereas for positive energies, one can always take the complex conjugate Herglotz alternative, this is not possible for negative energies. We have no way to obtain the correct path operator at these points. Fortunately, these energies are few and widely separated. In more realistic applications, the path operator is obtained numerically via Ewald's method and such difficulties do not arise. Wherever we have such difficulties we have indicated this with red arrow.

On the positive energy side we get as before, bands with smoother structures.

5.2: A PAIR MUFFIN-TIN POTENTIAL IN SUBSPACE I

Here we replace the region I by a pair of muffin-tin potentials of binary alloy types, i.e., $V_I(r) = -V_A$ or V_B with probabilities c and (1-c) respectively. We embed this in effective CPA medium described in section 5.1. We choose the member of the basis functions belonging to each well as

$$\chi_1(x) = 2 \frac{1}{N_1} (a_0 \chi_{1,0}(x) + a_1 \chi_{1,1}(x))$$

$$\chi_2(x) = 2 \frac{1}{N_2} (b_0 \chi_{2,0}(x) + b_1 \chi_{2,1}(x))$$

(5.2.1)

where $\chi_1(x)$ is the basis of the well with potential $V_1(r)$ and $\chi_2(x)$ with potential $V_2(r)$, as shown in figure 5.2. Here N_1 and N_2 are the normalization factors and $a_o = \exp(i\delta_{1,o})$, $a_1 = i\exp(i\delta_{1,1})$, $b_o = \exp(i\delta_{2,o})$, $b_1 = i\exp(i\delta_{2,1})$. We assume that the total wave function is $\psi(x) = A\,\chi_1 + B\,\chi_2$. Expanding trial wave functions in terms of equations (4.1.3a, 4.1.3b, 4.1.3d) we obtain

$$\chi_{1,o}(x) = R_{1,o}(r)\, Y_{1,o}(\hat{x})$$

with

$$\begin{aligned} R_{1,o}(r) &= \cos(kr-\delta_{1,o}) && -2r_s < r < -(r_s+r_o) \\ &= \cos \varkappa_1 r && -(r_s+r_o) < r < -(r_s-r_o) \\ &= \cos(kr+\delta_{1,o}) && -(r_s-r_o) < r < 0 \end{aligned} \qquad (5.2.2)$$

$$\chi_{2,o}(x) = R_{2,o}(r)\, Y_{2,o}(\hat{x})$$

with

$$\begin{aligned} R_{2,o}(r) &= \sin(kr-\delta_{2,o}) && 0 < r < (r_s-r_o) \\ &= \sin \varkappa_2 r && (r_s-r_o) < r < (r_s+r_o) \\ &= \sin(kr+\delta_{2,o}) && (r_s+r_o) < r < 2r_s \end{aligned} \qquad (5.2.3)$$

Similarly we can write the wave functions for l=1 partial waves.

Here $\varkappa_1^2 = (E-V_1)$, $\varkappa_2^2 = (E-V_2)$, $k^2 = E$. The phase shifts of these two wells for $l = 0,1$ partial waves can be obtained from the relations given in equations (5.2.4) :

$$\tan \delta_{1,o} = \frac{(\varkappa_1 \tan \varkappa_1(r_s+r_o)-k \tan (r_s+ r_o))}{(k + \varkappa_1 \tan k(r_s+r_o) \tan \varkappa_1(r_s+r_o))^{-1}}$$

$$\tan \delta_{1,1} = \frac{(k \tan \varkappa_1(r_s+r_o)-\varkappa_1 \tan (r_s+ r_o))}{(\varkappa_1 + k \tan k(r_s+r_o) \tan \varkappa_1(r_s+r_o))^{-1}}$$

$$\tan \delta_{2,o} = \frac{(\varkappa_2 \tan \varkappa_2(r_s+r_o)-k \tan (r_s+ r_o))}{(k + \varkappa_2 \tan k(r_s+r_o) \tan \varkappa_2(r_s+r_o))^{-1}}$$

$$\tan \delta_{2,1} = \frac{(k \tan \varkappa_2(r_s+r_o)-\varkappa_2 \tan (r_s+ r_o))}{(\varkappa_2 + k \tan k(r_s+r_o) \tan \varkappa_2(r_s+r_o))^{-1}}$$

(5.2.4)

In this basis the Hamiltonian has the 2x2 matrix representation with elements

$$H_{11} = EO_{11} + \frac{V_2}{N_1^2} \int_{r_s-r_o}^{r_s+r_o} dx\ \chi_1^*(x)\chi_1(x)$$

$$- \frac{2k}{N_1^2} \left[\cos(2kr_s+\delta_1^o) \sin(2kr_s+\delta_1^o) - \cos(2kr_s+\delta_1^1) \sin(2kr_s+\delta_1^1)\right]$$

$$- \frac{2}{N_1^2} \left[\frac{\cos^2(2kr_s+\delta_o)}{G_o(2r_s,2r_s)} + \frac{\sin^2(2kr_s+\delta_1)}{G_1(2r_s,2r_s)} \right]$$

$$H_{12} = E\ O_{12} + \frac{V_1}{N_1 N_2} \int_{-r_s-r_o}^{-r_s+r_o} dx\ \chi_1^*(x)\chi_1(x)$$

$$- \frac{2k}{N_1 N_2}\left[a_o^* b_o \cos(2kr_s+\delta_1^o)\sin(2kr_s+\delta_2^o) - b_1 a_1^* \cos(2kr_s+\delta_2^1)\sin(2kr_s+\delta_1^1)\right]$$

$$- \frac{2}{N_1 N_2}\left[\frac{a_o^* b_o \cos(2kr_s+\delta_1^o)\cos(2kr_s+\delta_2^o)}{G_o(2r_s,2r_s)} + \frac{b_1 a_1^* \cos(2kr_s+\delta_2^1)\sin(2kr_s+\delta_1^1)}{G_1(2r_s,2r_s)}\right]$$

$$H_{21} = EO_{21} + \frac{V_2}{N_1 N_2}\int_{r_s-r_o}^{r_s+r_o} dx\ \chi_2^*(x)\chi_1(x)$$

$$- \frac{2k}{N_1 N_2}\left[a_o b_o^* \cos(2kr_s+\delta_2^o)\sin(2kr_s+\delta_1^o) - b_1^* a_1 \cos(2kr_s+\delta_1^1)\sin(2kr_s+\delta_2^1)\right]$$

$$- \frac{2}{N_1 N_2}\left[\frac{a_o b_o^* \cos(2kr_s+\delta_1^o)\cos(2kr_s+\delta_2^o)}{G_o(2r_s,2r_s)} + \frac{b_1^* a_1 \cos(2kr_s+\delta_2^1)\sin(2kr_s+\delta_1^1)}{G_1(2r_s,2r_s)}\right]$$

$$H_{22} = E\,O_{22} + \frac{V_1}{N_2^2}\int_{-r_s-r_o}^{-r_s+r_o} dx\ \chi_2^*(x)\chi_2(x)$$

$$- \frac{2k}{N_2^2}\left[\cos(2kr_s+\delta_2^o)\sin(2kr_s+\delta_2^o) - \cos(2kr_s+\delta_2^1)\sin(2kr_s+\delta_2^1)\right]$$

$$- \frac{2}{N_1^2} \left[\frac{\cos^2(2kr_s+\delta_0)}{G_0(2r_s,2r_s)} + \frac{\sin^2(2kr_s+\delta_1)}{G_1(2r_s,2r_s)} \right]$$

(5.2.5)

and similarly the overlap matrix elements are

$$O_{11} = (4/N_1^2) \int_{-2r_s}^{2r_s} dr\ \chi_1^*(x)\ \chi_1(x)$$

$$O_{12} = (4/N_1N_2) \int_{-2r_s}^{2r_s} dr\ \chi_1^*(x)\ \chi_2(x)$$

$$O_{21} = (4/N_2N_1) \int_{-2r_s}^{2r_s} dr\ \chi_2^*(x)\ \chi_1(x)$$

$$O_{22} = (4/N_2^2) \int_{-2r_s}^{2r_s} dr\ \chi_2^*(x)\ \chi_2(x)$$

(5.2.6)

where the normalisation factors can be calculated from equation

(5.2.7)

$$N_1^2 = 4 \int_{-2r_s}^{2r_s} dr\ \chi_1^*(x)\ \chi_1(x)$$

$$N_2^2 = 4 \int_{-2r_s}^{2r_s} dr\ \chi_2^*(x)\ \chi_2(x)$$

(5.2.7)

The calculations of the integrals are done according to the criterion given in section 5.1.

The Green function of the effective medium on the interface S is given by equations (4.3.16b, 4.3.16c) and the path operator by equation (4.1.12). The density of states calculation is done according to the procedure given in section 5.1. Since $V_1(r)$ and $V_2(r)$ both have binary distributions, we have in all $2^2=4$ configurations, i.e., (AA,AB,BA,BB). Thus totally there are 4 sets of the 2x2 Hamiltonian and overlap matrix elements. Averaging over the configurations the density of states will be

$$n(r,E) = c^2 \ \mathrm{Im} \frac{O_{AA}}{EO_{AA}-H_{AA}} + (1-c)^2 \ \mathrm{Im} \frac{O_{BB}}{EO_{BB}-H_{BB}}$$

$$+ c(1-c) \ \mathrm{Im} \left[\frac{O_{AB}}{EO_{AB}-H_{AB}} + \frac{O_{BA}}{EO_{BA}-H_{BA}} \right]$$

(5.2.8)

5.2.1 : **RESULTS**

The negative density of states structures in 2CPA of 10%-90% compositions are in shown figure 5.3. Here all the CPA peaks of the same constituents splits into an anti-bonding and a bonding peak. This is the characteristic of 2CPA (Ahmed & Mookerjee 1990). The B_2 peak of 1CPA splits into B_2b and B_2a bonding and anti-bonding peaks whereas the A_2 peak into A_2b and A_2a respectively. The anti-bonding and bonding peaks are not well

separated. The bonding structure of these two peaks overlap to form a wide structure similar to the anti-bonding structure, they are C_1 and C_2 structures respectively. One can distinguish the overlap of the (A_{1b} , B_{1b}) structures in C_1 ,*i.e.*, bonding peaks of A_1 and B_1, but in C_2 we can not distinguish between the two anti-bonding structures (A_{1a} , B_{1a}) of A_1 and B_1. In this case all structures together form a single band with humps and peaks in between.

The positive energy structure is quite similar to the 1CPA case. It does not contain any extra interesting structure. So we have not drawn it separately.

We analyse the negative energy peaks of (50%-50%) composition of 2CPA in figure (5.4a) in comparison with figures (5.4b) and (5.4c) and (5.4d). Here all the bonding and anti-bonding peaks of AB, BB, AA overlap to form a wide band. The sharp peak C_2 comes from the contribution of all these AA, AB, BB sharp peaks which are denoted by C_2d, C_2b, C_2c in figures (5.4d, 5.4b, 5.4c) respectively. Then the structure drop slowly with a small hump C_3 which comes mainly from C_3d and C_3b peaks of AA and AB constituents as shown in figures (5.4d, 5.4b) respectively. The right most peak C_4 comes from the C_4b peak of the AB constituent as shown in figure 5.4b whereas the peak C_1 comes from the contribution of all AA, AB, BB constituents which are denoted by C_1d, C_1b and C_1c as shown in figures (5.4d, 5.4b, 5.4c) respectively, forming a wide structure.

Here also the change in the positive energy density of states is not prominent.

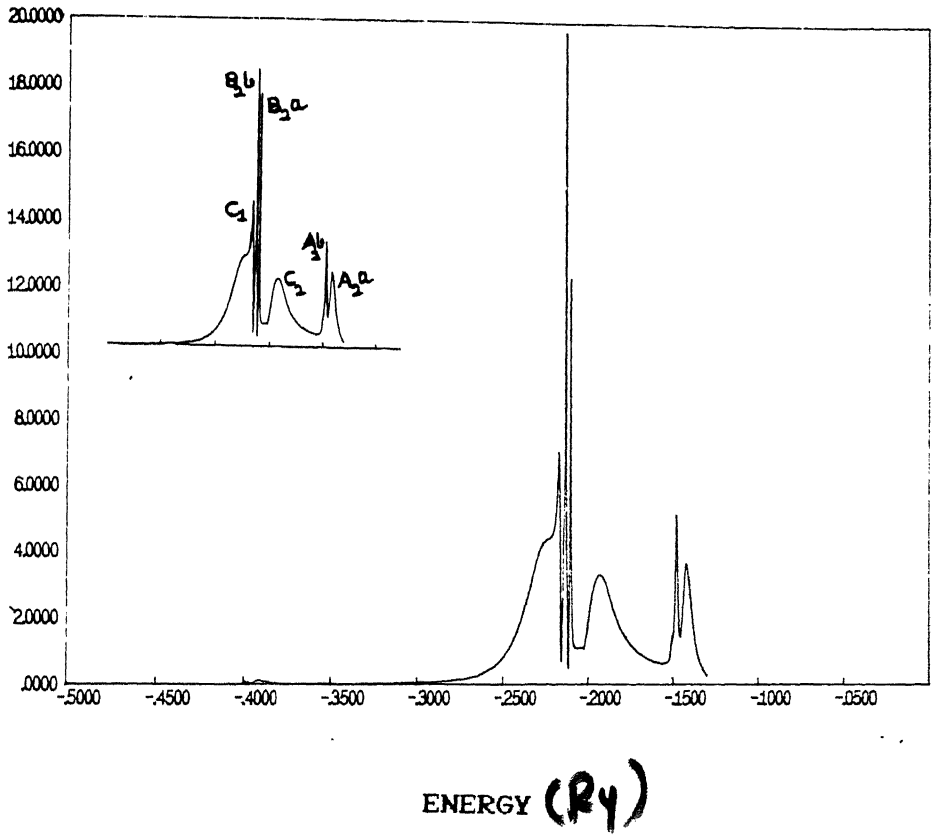

Figure 5.3 :2CPA, negative energy densities of states for V_A=-0.3 au, V_B=-0.5 au, and c=0.1.

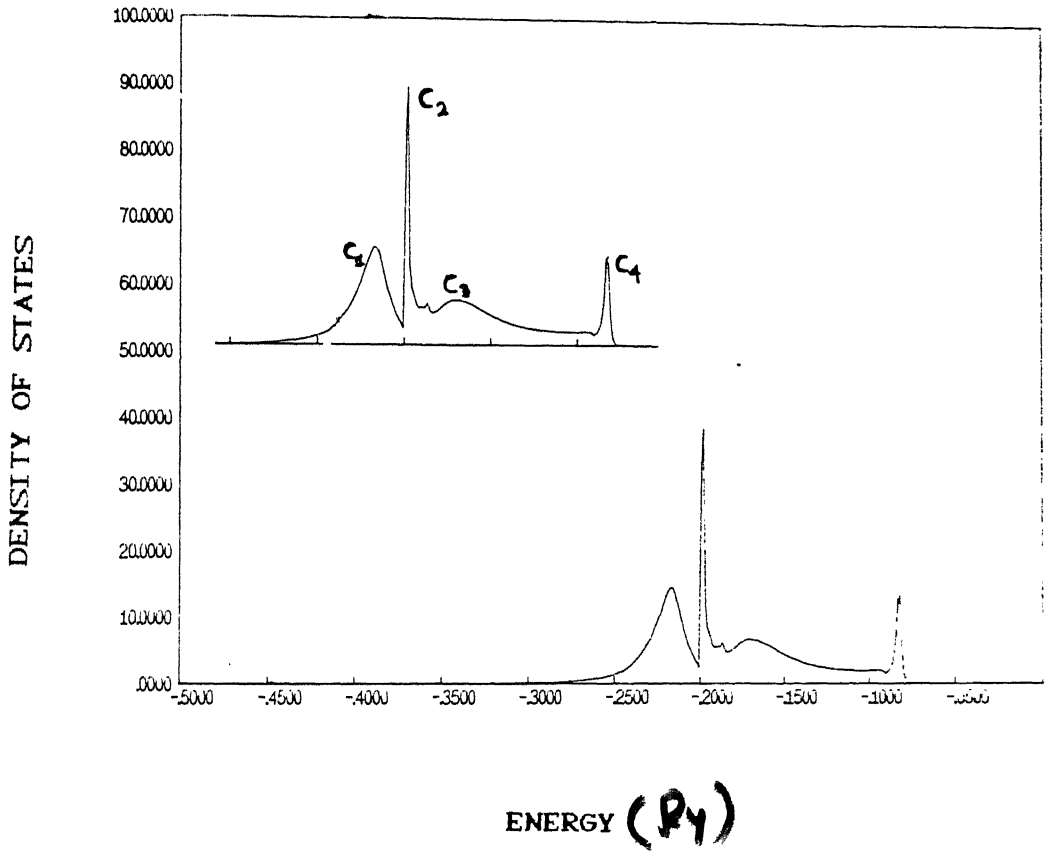

Figure 5.4a : 2CPA, negative energy densities of states for V_A=-0.3 au, V_B=-0.5 au, and c=0.5.

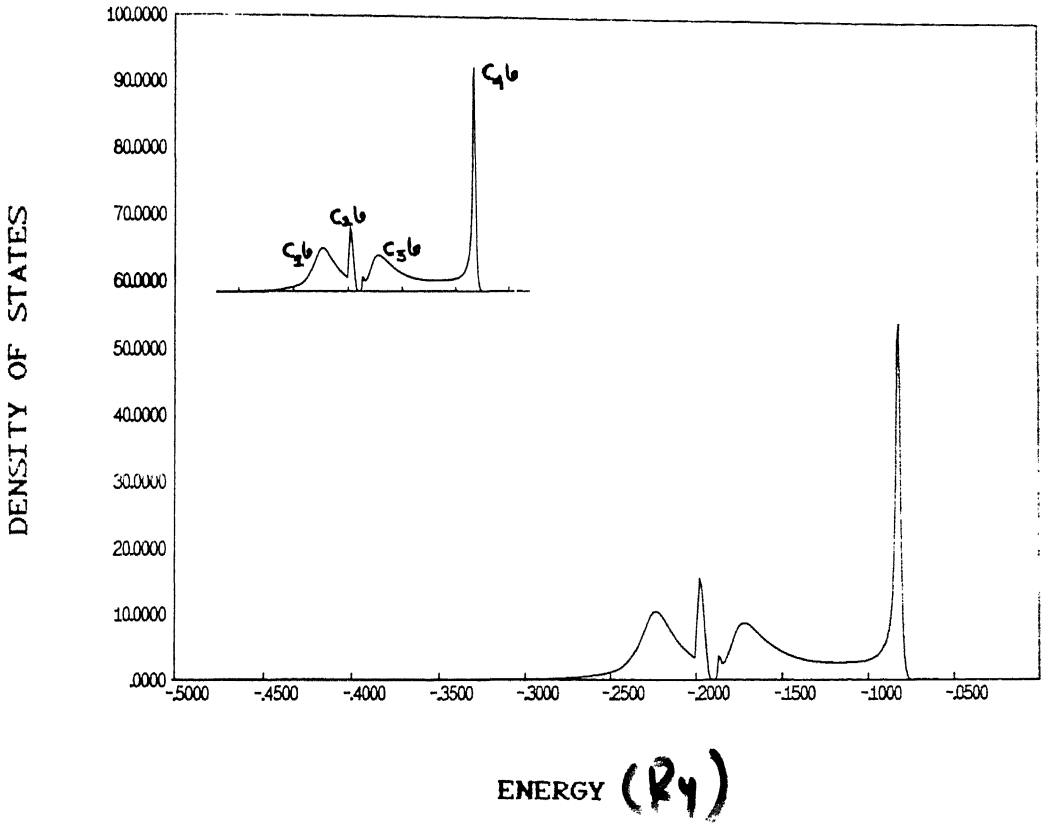

Figure 5.4b : 2CPA, negative energy densities of states of AB constituent for V_B=-0.5au, V_A=-0.3 au, and c=0.5.

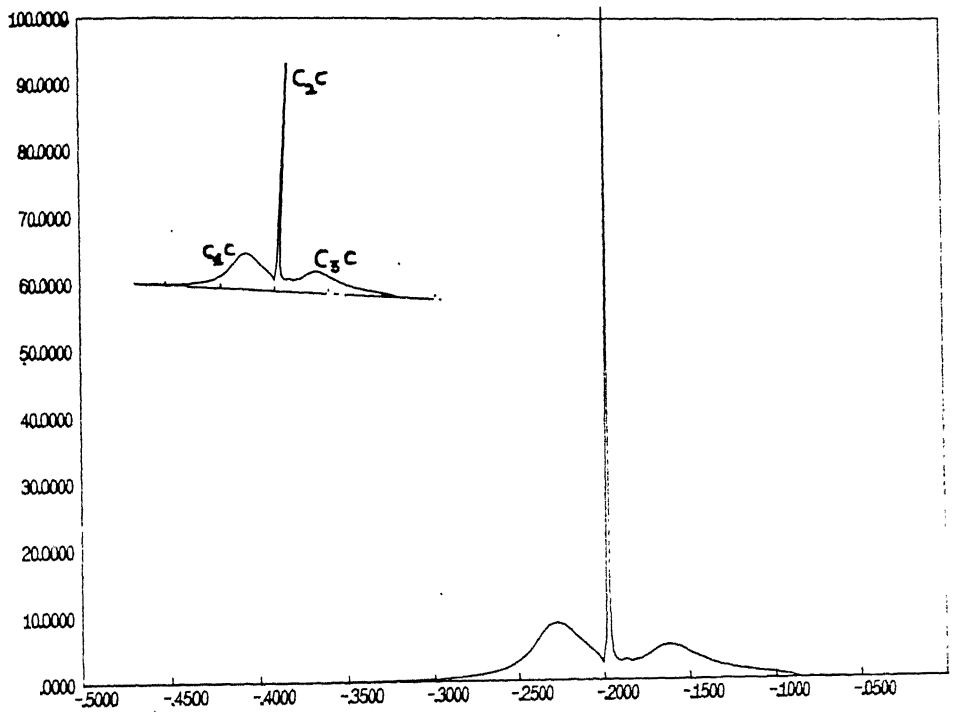

Figure 5.4c : 2CPA, negative energy densities of states of BB constituent for V_B=-0.5au, V_A=-0.3 au, and c=0.5.

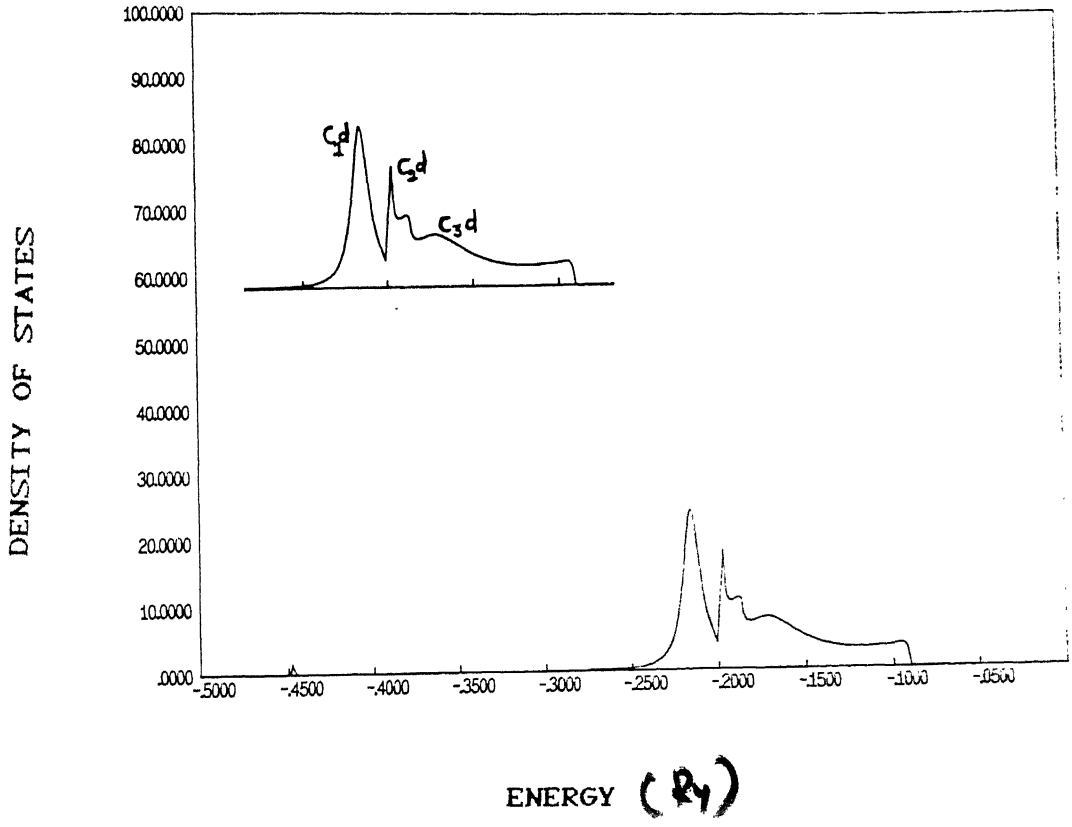

Figure 5.4d : 2CPA, negative energy densities of states of AA constituent for V_B=-0.5au, V_A=-0.3 au, and c=0.5.

CHAPTER VI

CONCLUDING REMARKS

" A surface potential is derived which can be added to the Schrödinger equation for a limited region of space, I, to embed it into a substrate. This potential, which is energy dependent and non local, can be found from the Green function for the bulk substrate. The results are based on a variational principle which gives the energy of a state in terms of the wave function in I. The embedded Schrödinger equation can be solved by a basis set expansion, for the wave functions of discrete states and the Green function in the continuum " .

—(Inglesfield 1981)

Our work is the alloy generalisation of the embedding ideas introduced by Inglesfield (1981). We have applied this formalism to calculate the local electron density of states of Coherent Jellium models, embedding different single muffin-tin potential wells in smaller space I, which is the muffin-tin sphere. For each type of potential we have done the calculation for three different concentrations of the alloy.

This formalism is developed in the most generalised form to take into account clusters of wells as well. Ahmed & Mookerjee (1989) applied this methodology to Coherent Jellium models, embedding a pair of muffin-tin potential wells. It is

interesting to note that the problem is very similar to the problem of a hydrogen like molecule in the subspace I immersed in a Coherent Jellium medium in subspace II. The various integrals involved in this case are the familiar two centre integrals in the finite subspace I.

The parameters they have chosen are the same as those reported by Mookerjee and Bardhan (1989) for one potential calculations. The principal new feature in this pair potential calculation is the splitting of the lower energy peak into bonding and anti-bonding structures. There is no such splitting in the higher energy peak, probably because the spread in this energy regime caused by the large imaginary part in the surface potential related to the inverse of the surface Green function 'K' makes the two split peaks not resolvable.

We may embed a cluster of muffin-tin potentials within the spherical region I (as shown in figure 6.1). The matrix representation of the Hamiltonian will then be in terms of a basis centred at each of the wells. This is reminiscent of the type of approach used in molecular electronic structure calculations with an atomic-like basis. The calculations will then involve multi-centre integrals. Apart from this complication, which has already been dealt with great detail in molecular calculations, the rest of the procedure is similar to what we have done.

We have also developed one dimensional analogs of the embedding formalism with the lattice structure left intact. We have calculated the required Green functions of the effective lattice using the KKR band theory in one dimension, developed by Butler (1976). Using this we have calculated the local electron density of states,embedding a single and a pair muffin-tin potential wells in an effective CPA medium. Since these are all model cases we have done the calculations for V_A = -0.3 au and V_B = -0.5 au and c = 0.5 and 0.1.

This formalism is an exact one. The only approximation used is the Coherent Potential Approximation to calculate the energy dependent non-local surface potential of the bulk substrate.

Let us now give a brief account of the further application of the embedding formalism. The one dimensional embedding formalism can be generalised to a three dimensional lattice where the Green function of the medium II can be obtained from the corresponding KKR theory. The difference here is that the three dimensional path operator can not be calculated analytically as in one dimension. It has to be calculated numerically using Ewald's or other related methods. Computer packages for the fcc and bcc lattices are available with us. Once this three dimensional formalism is obtained, calculation of the electronic properties of the real materials can be attempted.

This formalism can also be applied to study the effects of extended defects such as impurity clustering in an alloy and in liquid alloys, perhaps short-ranged order.

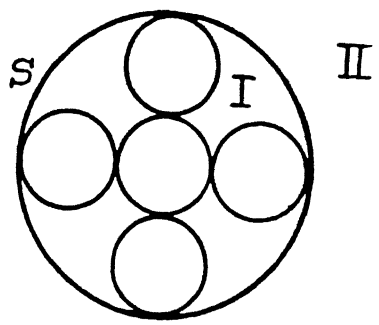

Figure 6.1 :A schematic diagram showing a cluster of spherically symmetric wells with a modified spherical boundary.

REFERENCES

Ahmed M. and Mookerjee A., (1989) J.Phys.: Condensed Matter : 1991-1998

Anderson P. W. , (1969) Phys. Rev 181 25

Butler W. H., (1976) Phys. Rev. B. 14

Butler W. H., (1973) Phys. Rev. B 8

Butler W. H., (1972) Phys.Lett. 39 , A203

Chandrasekhar S., (1960) Radiative Transfer (Dover New York)

Duscastelle F. and Gautier F. (1976) J.phys. F:Met Phys. 6 , 039

Elliot R. J., Krummhansl J. A. and Leath P. L,(1974)Rev.Mod.Phys. 46 ,465

Faulkner J. S.,Progress in material science, edited by T. Massalski (Pergamon, New York, 1982) vol. 27

Faulkner J. S. and Stocks G. M.(1980) Phys.Rev.B 21 , 3222

Ganguli B.,(1989) Ph.D thesis (IIT Kanpur, Unpublished)

Gonis A., Stocks G.M., Butler W.H. and Winter H. (1984) Phys.Rev. B 29 , 555

Gray L. J. and Kaplan T. (1976a) J.Phys. C:Solid State Phys. 15 303, L 483

Gray L. J. and Kaplan T. (1976b) Phys. Rev. B. 14 , 3462

Gyorffy B. L. and Stott M.J.,Solid State Communication

Gyorffy B. L. and Stocks G.M., (1980) J.Phys. F 10 , L 321

Gyorffy B. L. , (1972) Phys. Rev. B. 5 , 2382

Heine V. (1980) Solid State Physics, Vol. 35 (Academic Press, Inc. New York)

Haydock R. , (1987) "Electronic Band Structure and It's Applications", edited by M. Yussouff, Lecture notes in Physics 283(Springer-Verlag)

Haydock R.,Heine V. & Kelley M. J. ,(1972) J. Phys. C 5 , 2845

Inglesfield J.E.,(1981) J. Phys. C :Solid State Phys. 14 , 3795

Inglesfield J.E.,(1972) J. Phys. F: Met. Phys. 2 , 878

Inglesfield J.E.,(1971) J. Phys. C: Solid State Phys. 4 , L 14

Jackson J. D., Classical Electrodynamics (second edition) (Wiley Eastern Delhi,Ltd.)

Kelly M.J. (1980) Solid State Phys., Vol 35 (Academic Press ,Inc.New York)

Kirkpatrick S.,Velicky B. and Ehrenreich H. (1970) Phys. Rev. B 1 , 427

Kohn W. and Rostoker N., Phys. Rev. 94 , 1111 (1954)

Korringa J. , (1947) Physica 13 , 392

Kumar N. and Jayannavar A.M , (1986) J. Phys. C 19 , 5513

Kumar N. and Jayannavar A.M , (1985) Phys. Rev. B 32 , 3345

Kumar V., Mookerjee A. and Srivastava V.K., (1982) J. Phys. C Solid States Phys. 15 , 1939

Leath P. L. , (1972) Pyhs. Rev. B5 , 1643

Leath P. L., (1970) Phys. Rev. B2 , 3078

Leath P.L., (1968) Phys. Rev. 171 , 725

Luban M. and Nudler-Blum B., (1977), J.Math. Phys., 18 , 1977

Mills R.and Ratanavaranaksa R. , (1978) Phys. Rev. B 18 , 5291

Mookerjee A., (1975a) J.Phys. C 8 , 24

Mookerjee A., (1975b) J.Phys. C 8 ,1524

Mookerjee A., (1975c) J. Phys. C 8 , 2688

Mookerjee A., (1973a) J.Phys. C 6 , L205

Mookerjee A., (1973b) J.Phys. C 6 , 1340

Mookerjee A. and Bardhan S., (1989) J.Phys.Condensed Matter 1,509

Muller-Hartmann E , (1973) Solid State Communication 12 , 1269

Nickel B. G. & Krummhansl J. A., (1971) Phys.Rev. B 4 , 4357

Nickel B. G. & Butler W.H. , (1973) Phys. Rev. Lett. 30 , 373

Schiff L. I., (1968) Quantum Mechanics, 3rd edition (McGraw - Hill Kogakusha, Ltd.,Tokyo).

Soven P., (1967) Phys. Rev. 156 , 809

Soven P., (1970) Phys. Rev. B 2 , 4715

Srivastava V. K. , (1982) Ph.D. thesis (IIT Kanpur, unpublished)

Tsukada M., (1969) J. Phys. Soc. Japan. 26 , 684

Thakur P. K., (1980) Ph.D thesis (IIT Kanpur, unpublished)

Yonezawa F. and Matsubara T., (1966) Prog Theor Phys 35 , 357,759.

S.S.A. Razee, S.S. Bajpai, R. Prasad and A. Mookerjee, Phys. Rev. B 42, 9391 (1990)